GL-TR-89-0338

AD-A226 814

Attenuation of Seismic Waves in the Near-Source Region

Leon Knopoff

University of California
405 Hilgard Avenue
Los Angeles, CA 90024-1567

DTIC
ELECTE
SEP 25 1990
D

14 December 1989

Final Report
17 February 1987-16 February 1989

GEOPHYSICS LABORATORY
AIR FORCE SYSTEMS COMMAND
UNITED STATES AIR FORCE
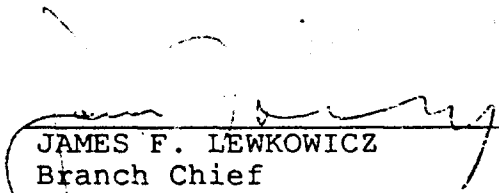HANSCOM AIR FORCE BASE, MASSACHUSETTS 01731-5000
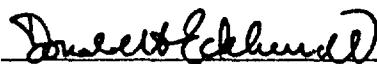
This technical report has been reviewed and is approved for
publication.

JAMES F. LEWKOWICZ
Contract Manager
Solid Earth Geophysics Branch
Earth Sciences Division

JAMES F. LEWKOWICZ
Branch Chief
Solid Earth Geophysics Branch
Earth Sciences Division

FOR THE COMMANDER

DONALD H. ECKHARDT, Director
Earth Sciences Division

REPORT DOCUMENTATION PAGE

Form Approved
OMB No. 0704-0188

1a. REPORT SECURITY CLASSIFICATION	1b. RESTRICTIVE MARKINGS
Unclassified	N/A

2a. SECURITY CLASSIFICATION AUTHORITY	3. DISTRIBUTION/AVAILABILITY OF REPORT
N/A	Approved for public release;
2b. DECLASSIFICATION/DOWNGRADING SCHEDULE	distribution unlimited
N/A	

4. PERFORMING ORGANIZATION REPORT NUMBER(S)	5. MONITORING ORGANIZATION REPORT NUMBER(S)
	GL-TR-89-0338

6a. NAME OF PERFORMING ORGANIZATION	6b. OFFICE SYMBOL (If applicable)	7a. NAME OF MONITORING ORGANIZATION
Regents of the University of California (IGPP)		Geophysics Laboratory

6c. ADDRESS (City, State, and ZIP Code)	7b. ADDRESS (City, State, and ZIP Code)
405 Hilgard Avenue Los Angeles, California 90024-1567	Hanscom Air Force Base Massachusetts 01731-5000

8a. NAME OF FUNDING/SPONSORING ORGANIZATION	8b. OFFICE SYMBOL (If applicable)	9 PROCUREMENT INSTRUMENT IDENTIFICATION NUMBER
Geophysics Laboratory	GL/LWH	F19628-87-K-0020

8c. ADDRESS (City, State, and ZIP Code)	10. SOURCE OF FUNDING NUMBERS			
Hanscom Air Force Base Massachusetts 01731-5000	PROGRAM ELEMENT NO	PROJECT NO	TASK NO	WORK UNIT ACCESSION NO.
	61101F	7A10	DA	CW

11. TITLE (Include Security Classification)

Attenuation of Seismic Waves in the Near-Source Region

12 PERSONAL AUTHOR(S)
Leon Knopoff

13a. TYPE OF REPORT	13b. TIME COVERED	14. DATE OF REPORT (Year, Month, Day)	15. PAGE COUNT
Final	FROM 2/17/87 TO 2/16/89	December 14, 1989	64

16 SUPPLEMENTARY NOTATION

N/A

17. COSATI CODES			18. SUBJECT TERMS (Continue on reverse if necessary and identify by block number)
FIELD	GROUP	SUB-GROUP	Attenuation, Fatigue Crack Growth, Stress Corrosion

19. ABSTRACT (Continue on reverse if necessary and identify by block number)

We consider a model of elastic wave propagation through a material permeated by a dilute ensemble of cracks. The excitation strains are large enough to cause the cracks to grow either by fatigue or by stress corrosion. As the cracks grow, energy is removed from the excitation. The dominant mechanism of growth, and hence for absorption, is creep in the slip-weakening zone at the edges of the cracks. Because of non-linearity, the attenuation in the time domain in this case is significantly waveform dependent. For harmonic excitation and narrow bandwidth detection, 1/Q varies as the cube of the excitation amplitude and is independent of the frequency. For broad band impulsive excitation and detection, an equivalent transfer function for the attenuation has a Q which varies as the first power of the frequency for low frequencies, both for simulated explosion and extended noisy waveshapes.

20 DISTRIBUTION/AVAILABILITY OF ABSTRACT	21. ABSTRACT SECURITY CLASSIFICATION
☒ UNCLASSIFIED/UNLIMITED ☐ SAME AS RPT. ☐ DTIC USERS	Unclassified

22a. NAME OF RESPONSIBLE INDIVIDUAL	22b TELEPHONE (Include Area Code)	22c OFFICE SYMBOL
James F. Lewkowicz	(617) 377-3222	GL/LWH

DD Form 1473, JUN 86   *Previous editions are obsolete.*   SECURITY CLASSIFICATION OF THIS PAGE

Table of Contents

I. Introduction

The phenomenology of attenuation of elastic waves in solids as derived from both laboratory and geophysical measurements has been summarized by Knopoff (1964). Under conditions of harmonic excitation, the laboratory data support, to lowest order, a Q that does not depend on the frequency. The seismological data support a similar conclusion; but rather more roughly so: interpretations of free oscillation data and body and surface wave propagation studies give Q's for S-waves or Rayleigh waves that range roughly from 100 to 1000, over a period range from about 1 sec to 1000 sec. But in the case of terrestrial measurements, the measured values of Q are hardly estimates of homogeneous samples; instead they represent averages over different parts of the earth; the values at the longer periods are weighted averages across the entire mantle, and those at the shorter periods are averages in the near surface regions. Since the different estimates sample different parts of the earth in each case, it is not clear what the detailed frequency dependence of Q might be for any localized portion of the earth's interior, but the narrowness of the range of Q's suggests that Q probably does not vary too much with frequency in any broad depth range of the mantle. The Q's for P-waves in the core are very high, and do not concern us here.

The field data are perforce taken from observations at very much longer wavelengths than in the laboratory; strains in usual field measurements of seismic waves are much smaller than a suggested threshold between the linear and nonlinear regimes of about 10^{-6} (McKavanagh and Stacey, 1974). On the other hand, the laboratory

measurements are often made at strains larger than 10^{-6}. It is therefore plausible that two different physical mechanisms may have to be invoked to understand the two sets of experimental attenuation results. Attenuation in the small strain regime of mantle wave propagation is well understood due to the significant contributions of Anderson and Minster and colleagues (see for example, Anderson, et al., 1976; Minster, 1980; Minster and Anderson, 1980) who have identified the importance of the motions of dislocations and dislocation networks, and especially relaxation processes associated with such motions.

Between the source of large earthquakes or explosions and the small-strain regime of the far-field in the earth, there are several regions where stress wave propagation is patently non-linear. In order of decreasing strain, these are- after the source region itself- 1) a region where the physics is dominated by the growth of numerous fractures due to the high stress field, even leading to spallation and fragmentation in the nearest source regions, 2) a region dominated by passive scattering from numerous cracks where the theory of scattering by dilute concentrations is inappropriate, and 3) the grain boundary sliding regime. The last of these is of course followed by the linear region, extending to the greatest distances.

In this report we consider the problems of attenuation of stress waves in the first of these regions, namely that close to the near-source region of an explosion, or in the domain of large ground motions due to a strong earthquake where the dynamic strains are large. The problems of attenuation in the second region have not been well

studied as yet, although the problems of scattering of body waves from penny-shaped cracks has been analyzed to the second order in concentration (Hudson, 1986; Hudson and Knopoff, 1989); such studies have not been carried out to higher order concentrations of cracks. In this research we have also attacked the problems of attenuation due to grain-boundary sliding, and have found that the early model of Knopoff and MacDonald (1956) gives a satisfactory description of the behavior of materials in this strain range. As remarked, in this report we focus on the problems of crack growth under conditions of large stress excitation.

The outermost parts of the earth are permeated by fractures in abundance and we look to the dynamical interaction of such cracks with the (large) stress field to understand the absorption and propagation of the stress waves. While we can consider a crack to be an aggregate of point dislocations, the description of motions of such aggregates is rather difficult. Grain boundaries also represent aggregates of dislocations whose response to external stresses are difficult to treat because of their collective properties. It is more appropriate to consider finite cracks, including grain boundaries considered as cracks with irregular walls, as macroscopic objects with a dynamic response to stress excitation given by more-or-less classical models, rather than considering them from the point dislocation point of view.

As a generalization, Knopoff and MacDonald (1956) and Knopoff (1964) have shown that if Q is truly frequency independent over a broad range of frequencies for a wide variety of materials, the process

causing the attenuation must be a non-linear one; the argument, although elementary, will not be repeated here. However, we do not argue for Q independent of the frequency in the stress range that we are considering here. This relationship, to lowest order, is more or less valid in the experimental range of strains up to about 10^{-5}, but the upper end of the range is more appropriate to the grain-boundary sliding problem. While there are many measurements of deformation response, there are few if any data on attenuation in the strain range corresponding to crack growth. Almost all, if not all, of the laboratory data on Q measurements in the harmonic regime are made on compact, relatively unfractured rock. Even those few measurements of attenuation that have been made on highly fractured rock or soil samples, are rarely made in the strain range that would cause cracks to grow. Thus the results reported below are theoretical. As remarked, the strain range of applicability of these calculations corresponds to the very near field of explosions or large earthquakes. In the present case, we are without adequate controlled experimental guidance.

Before taking up the problems of crack growth response under the influence of a strong, transient stress wave, we consider the growth of cracks under periodic excitation. The failure of aircraft structures under continuous flexing, i.e. loading and unloading, is a prominent contemporary example of such material response. In this model of failure, pre-existing cracks grow under the influence of the oscillatory stress; ultimately these cracks fuse with one another to make large cracks and when the dimensions of a crack become comparable to the dimensions of the specimen, catastrophic failure is the

consequence. This type of behavior is called fatigue crack growth in the engineering literature. We consider only the problem of the growth of isolated cracks, and bypass the problems of crack interactions; the latter problem for the case of cracks in a static external stress field has recently been considered from a quasistatic growth point of view by Yamashita and Knopoff (1989), but the case of dynamic stress excitation has not been discussed, as far as we know. Since growth involves the breaking of bonds at the tip or tips of a crack, it is plausible to suppose that if the change in crack length of an isolated crack is very small, the amount of energy absorbed out of the seismic wave ΔE is the same on each cycle and therefore yields a ratio of $\Delta E/E = 2\pi Q^{-1}$ that is independent of the frequency, where E is the peak energy stored. We investigate the validity of this presumption.

A second model of crack growth involves stress-corrosion, i.e. the hydrolytic weakening of silicate bonds at crack tips, which can generate crack growth/extension. We will see that this process will give results that are similar to those from fatigue crack extension.

II. Fatigue Crack Growth

We consider non-linear models of attenuation caused by crack growth under external time-dependent stress excitation. In the case of harmonic stress excitation, our goal was to construct a model that would be appropriate in the very large strain regions that might be found at very short range from explosions or earthquakes. As noted, we are not aware of laboratory data to support this ambition in the crack growth range of strains. The conditions of crack growth depend on the stresses at the crack tips, which are of course intensifications of the large-scale field due to the presence of the cracks.

Two generic models of crack growth can be considered, namely fatigue crack models and stress-corrosion models. In the fatigue crack case, the large stress concentration near a crack tip induces a plastic, or slip-weakening zone in the vicinity of the tip (Barenblatt, 1962). Beyond the outer boundary of the plastic zone, the material is presumed to be perfectly elastic. For purposes of pedagogy, the boundary between the elastic and plastic regions will be assumed to be sharp. The degree of weakening in the plastic zone increases as we approach the crack tip; at the crack itself, the stress has dropped to such a low level that dynamical sliding can take place. A slip-weakening model has been applied to dynamical theories of fracture as well as to quasistatic crack growth problems in seismology by a number of authors (Ida, 1972; Palmer and Rice, 1973; Andrews, 1976; Rice, 1980; Kostrov and Das, 1982, Chen and Knopoff, 1986 a,b).

-6-

The slip-weakening model is amply buttressed by results from microscopic examination of and macroscopic deformation experiments on metals and rocks. While there is (again) ample evidence for the presence of non-linear viscous creep in highly stressed rocks especially at normal and high temperatures and in the presence of fluids (see Griggs, 1940; Griggs and Handin, 1960; and many others), it must be remarked that at liquid nitrogen temperatures and under very dry conditions, the deformation proceeds by microcracking ahead of a main crack (Hoagland, et al., 1973); Hoagland et al. have gone to special effort toward "eliminating plastic deformation". However under normal environmental circumstances, plastic deformation in a slip-weakening zone is an appropriate model to describe the response in the region ahead of an existing stressed crack. Indeed, the deformation of an aggregate of microcracks in the deformed zone ahead of a crack tip, with increasing density of microcracks toward the crack tip, may also have an equivalent plasticity-slip-weakening continuum description. In the strain range of interest, we will take it that slip-weakening, whether it be associated with plasticity due to slip band formation or microcracking, will be the appropriate description of the deformation in the zone immediately adjacent to the crack tip.

In fatigue crack models, the amount of extension ΔL is calculated from Paris' Law, which is widely discussed (Paris. 1964: Rice. 1967: Cherepanov, 1979; and many others).

$$\Delta L \sim (K - K^*)^4 \qquad (1)$$

where K is the stress intensity factor at the crack tip and K^* is the stress intensity factor at which growth begins. This relation has been verified experimentally many times over under conditions of monotonic loading, but mainly on samples subjected to tensile stresses. It is plausible to assume that these results also apply to shear cracks. Differences in the response between these two modes of excitation arise in the case of oscillatory loading; the sample is in tension for one-half of a sinusoidal cycle of loading, and on the simplest picture in the case of tensile-compressional loading, accelerated growth will takes place during the quarter cycle for which the tensile stresses are increasing. In the case of a crack under shear loading, it is the absolute stress that is involved in crack growth; the increase of stress that initiates and promotes growth takes place on alternate quarter cycles. Our examples will be given for tensile cracks only for the purposes of clarity. We do not believe the results will be negated for shear cracks, because the stress singularity at the edge of a shear crack has the same relationship to external stress and to crack geometry as in the case of a tensile crack. Further the nature of the plastic deformation in both the rock deformation shear experiments (Griggs, 1940 and successors) and tensile deformation in metals experiments shows similar properties, except for the time constants, which are scaling factors in the calculations.

The relation (1) can be derived rather simply as follows: The slip-weakening zone extends from the crack tip to the elastic-plastic boundary. On a continuum theory, the energy required to break the bonds at the crack tip itself is proportional to the sliding friction;

the strength of the material at the crack tip is zero if the sliding friction is zero, an assumption we make henceforth. The strength in the plastic zone drops to zero at the crack tip because of accumulated damage or slip in the zone. Thus all of the energy required to advance the edge of the crack must go into advancing the plastic zone of deformation and to increasing the deformation in the zone. (We assume here that the rate of advance of the crack is slow enough that radiation effects can be neglected.) The size of the plastic zone is estimated as follows: Let the elastic-plastic boundary be defined by a critical yield stress, σ_Y. The stress in the vicinity of the crack tip falls off with distance x from the where $K \sim \sigma L^{1/2}$ is the stress intensity factor, L is the length of the crack, and σ is the external applied stress (Fig. 1). Thus the radius R of the plastic zone is proportional to the square of the applied stress, $R \sim (\sigma/\sigma_Y)^2 L$. The energy per unit length needed to create a plastic zone can be estimated by the area of the zone, and thus is proportional to L^2, and hence to K^4. The remainder of our discussion concerns, in one form or another, the appropriateness of relation (1), and especially the significance of the quantity K^*.

With regard to the deformation response to a more-or-less simple stress impulse such as might be expected in the near field of an explosion, the above description probably suffices. The cracks grow under the influence of the increasing stress. (Chen and Knopoff (1986) have discussed the growth of simple cracks under a large stress in the presence of a slip-weakening zone in a linear viscoelastic medium; it is unlikely that the viscoelastic property will be linear in nature in
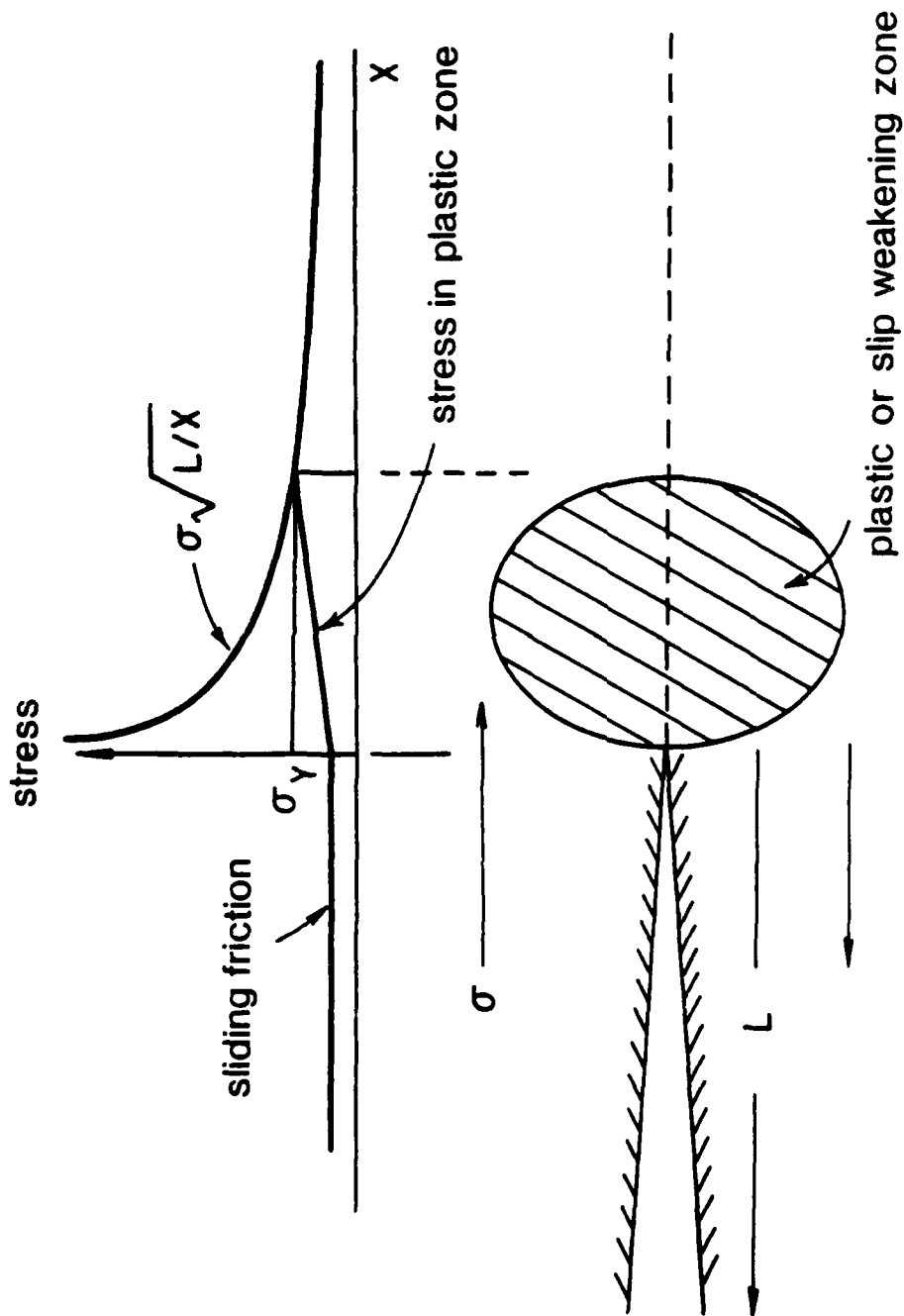
Figure 1. Schematic diagram of crack-tip neighborhood showing plastic/slip-weakening zone. Elastic-plastic boundary is determined by the locus where the stress concentration near the crack tip is equal to the yield stress of the material. The curve of stress in the plastic zone connects the plastic-zone boundary with the frictional stress at the crack tip; precise details of this curve are given by an equation of state for the plastic zone. If the external stress is removed, the strength in the plastic zone becomes equal to the stress shown; the strength outside the plastic zone is σ_Y.

the slip-weakening zone.)   As for the response of cracks to the waning part of a $\underline{simple}$ $\underline{stress}$ $\underline{impulse}$, we will show that it is probably inappropriate to assume that the lengths of the cracks are frozen when the stress maximum is reached and hence it is inappropriate to assume that the response during the reduction of the stress after the maximum is reached is of no concern to us. To discuss the problem of the response to both oscillatory and impulsive stresses, we have to describe in detail the nature of the deformation in the slip-weakening zone.

The zone of plasticity/slip-weakening in metals is a complex region whose microscopic properties suggest that the deformation takes place along a series of steps formed by the offset of relatively coherent slabs of matter, as though the material had been sheared along along well-defined planes (see Lin, 1977, for example; also see Fig. 2). In metals, the thickness of these slabs may be no more than a few microns. Many of the features of the deformation are similar for rocks, including the presence of slip lamellae, twinning, etc. Microcracking ahead of cracks can also occur. We have stated that we believe that microcracking may have a continuum description similar to the one we use here for plasticity. In any case the plasticity model is an effort to override the microscopic details of deformation with a continuum theory. We assume that the continuum description of the plastic state of metals is appropriate for rocks as well.

SURFACE

SLIP BAND

(a)

$\dashv 10\mu \vdash$ (b)
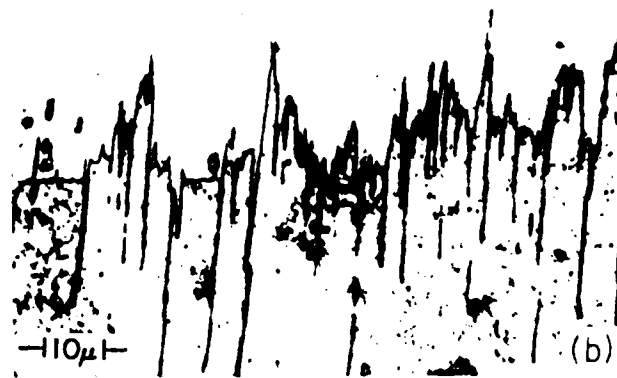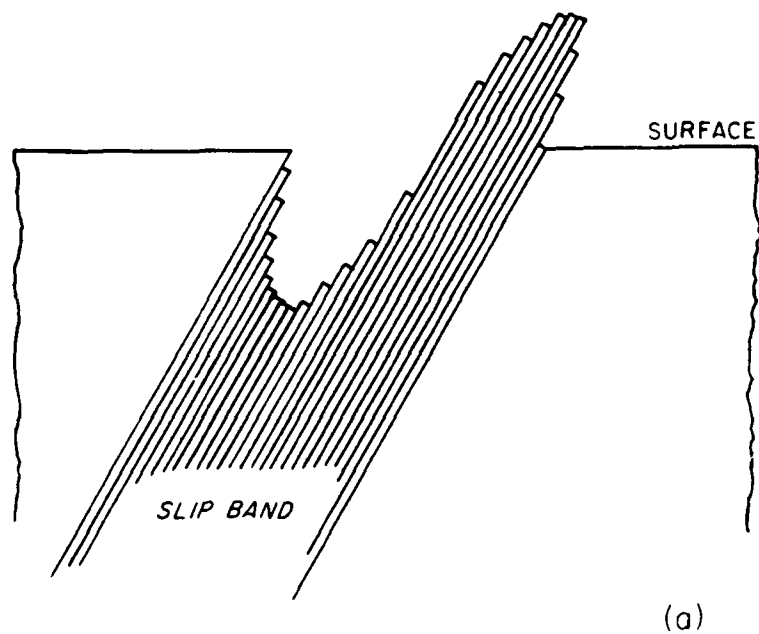
Courtesy W. A. Wood

—Notch-peak geometry which develops at slip bands: (a) schematic representation.
(b) *taper section of copper after* 2×10^5 *cycles at 0.003 shear strain in alternating torsion.*
Taper magnification of 20.

Figure 2 (a-e) Photomicrographs and schematic cross-sections of copper, showing slip-banding(from Grosskreutz, 1971).

(c)

SURFACE

SLIP BAND

MATRIX
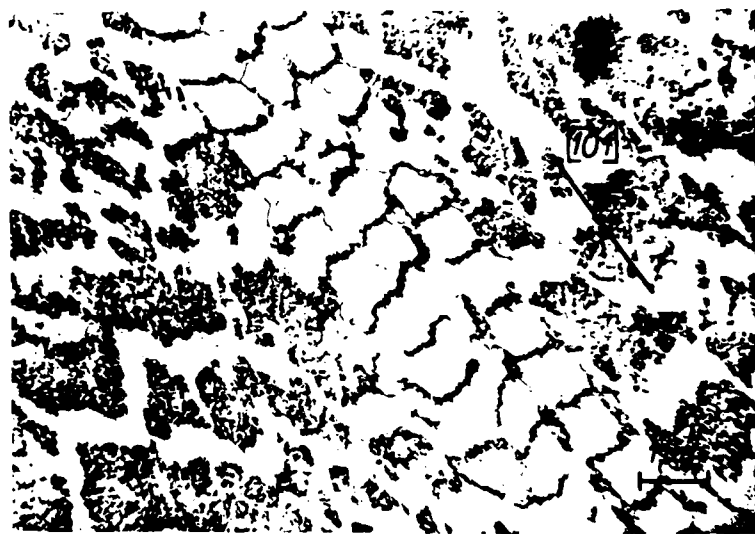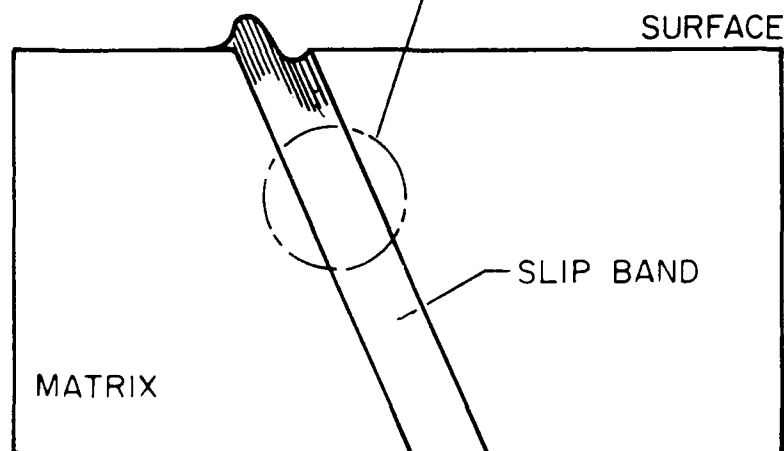
(d) Dislocation cell structure in slip bands of fatigued copper (Lukas, Klesnil, and Krejci, Ref 16)
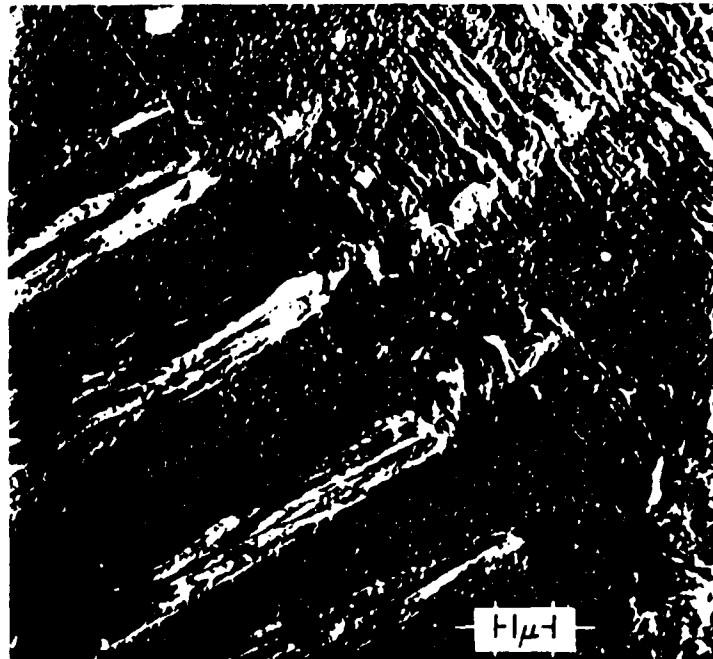
(e) *Surface slip bands on fatigued copper (electron replica)*

III. Fatigue Cracking: The Cyclic Loading Problem

The interpretation of Paris' Law may be clearer for the case of a simple pulse than for cyclic loading, but the cyclic problem has certain perplexing features that will ultimately bear on the pulse problem as well. In one version it can be argued that, as a new peak in cyclic stress is reached, "a new plastic zone forms superimposed over the previously formed zones" (Paris, 1964) due to the theoretical infinite stress at the crack tip at $x = 0$. Thus Paris, Cherepanov (1979) and others argue that K^* is the value of the local stress minimum, and/or that cracks begin to grow after the stress has reached its minimum, and that the amount of crack growth is proportional to the fourth power of the difference between a maximum in stress and its preceding minimum. Under this model, the crack grows on each successive cycle of stress, with reduced memory of the deformation on preceding cycles of the stress, since the plastic zone must be a new one on each stress cycle; the crack always grows into a zone of elastic material at the start of any phase of increasing stress. Thus the Paris/Cherepanov et al. model asserts that the amount of crack growth per cycle is proportional to the fourth power of the difference between the maximum stress on any cycle and the last preceding minimum.

However this model, argues for the disestablishment of the plasticity upon even a partial reduction of the load stress, in order that each succeeding cycle of increasing stress initiate a new episode of deformation. As an illustration of the difficulty with this model, consider the two hypothetical loading sequences of Fig. 3. In the
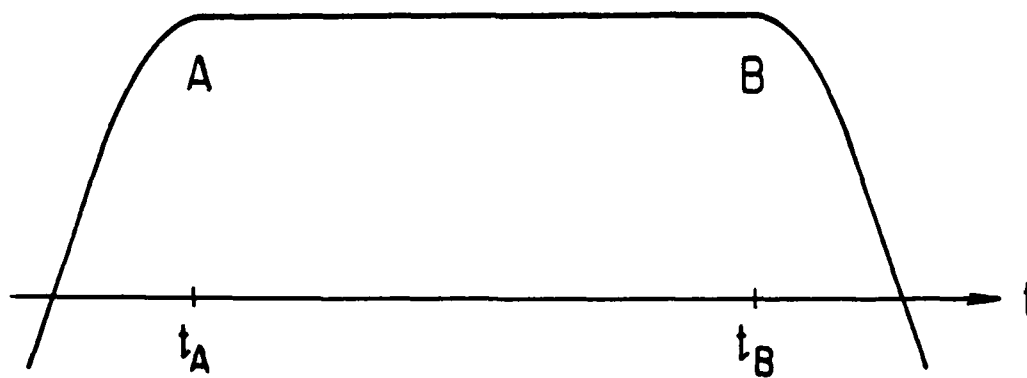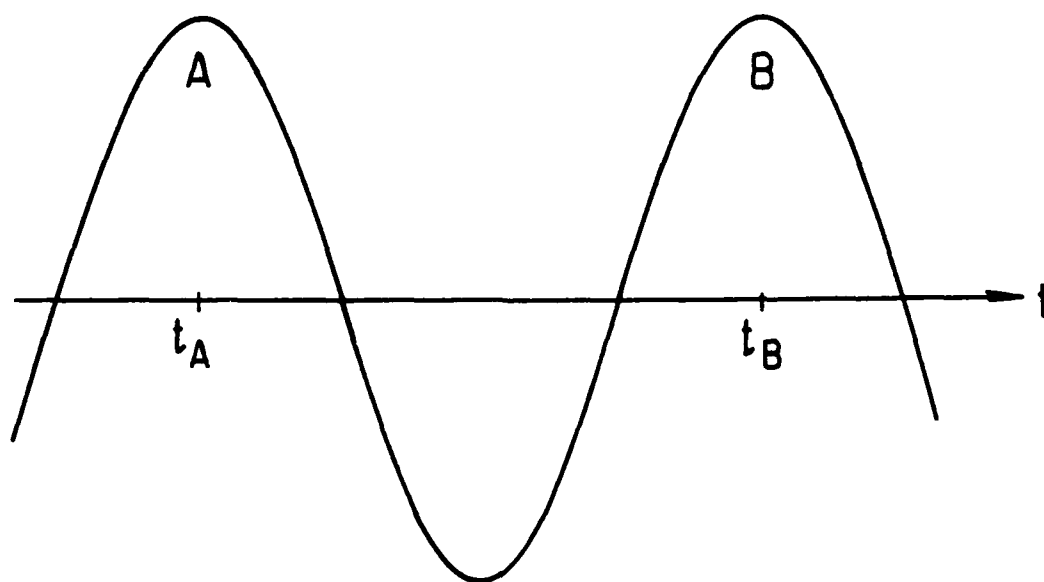
Figure 3: Two hypothetical loading curves.

first case, it is an experimental fact that the crack grows when the second maximum is reached. In the second, according to the model, the crack cannot grow between the two times (t_A, t_B) because the stresses in the plastic zone are in equilibrium with the strength distribution given by the constitutive equation for the slip weakening zone and the size of the plastic zone, i.e. the crack cannot grow because the stresses never were decreased. Therefore, we conclude that the ability of the crack to grow on the next application of the maximum stress must depend on the way in which the plastic zone behaves in the waning part of the stress cycle, and that the conventional model must be modified. It is more likely that the damage resulting from the earlier stages of deformation has a strong influence on damage history as the later loading history evolves.

Weertman (1978, page 290) offers a solution to the problem: "during each stress cycle, the material ahead of a fatigue-crack tip is progressively "weakened". The material closest to the tip is weakened the most because it has been subjected to more cyclic plastic deformation than the material farthest from the tip, which has just entered the plastic zone. In each stress cycle, the crack tip passes through the most weakened and damaged material and comes to a stop in less damaged material. Subsequent stress cycles in turn increase the damage of this material and permit further crack advance." Weertman then derives an Accumulated Damage Theory.

We focus on Weertman's use of the word "during", which we believe attacks directly the question of why the stress pattern in the plastic zone should not be exactly the same at one peak of a cyclic excitation as on the next. A detailed explanation of the process bears on the issue of the attenuation of stress waves in the fatigue crack regime. We restate the problem: Why should the damage be increased in the time interval between successive peaks of the stress cycle in a perfectly sinusoidal stress excitation so that the crack will grow when the next peak occurs? If the strength in the slip-weakening zone were perfectly adjusted to match a given maximum in stress, it would be in the same configuration at the time of the next maximum as well, and thus there is no mechanism to compel the crack to grow. Thus, although the Paris model fails to offer a sound physical reason for deflation of the plastic zone and replacement by a strong elastic region, we must present an argument for accumulation of damage in the time interval between successive peaks of a perfectly sinusoidal applied stress.

All of this argues against a static theory of fatigue crack growth, even though the process of deformation may be taking place quasistatically. The differentiation of equation (1) with respect to time

$$\frac{dL}{dt} \sim \frac{d(K-K^*)^4}{dt} \tag{2}$$

will lead to incorrect results because of the failure to account for processes that depend on loading and unloading histories. In other words, a statics theory such as (1) omits certain important

time-dependent terms even though the rates of deformation we are considering are slow.

To get around the difficulty, we develop a model for the increase of the damage, i.e. a lowering of the strength, in the time interval between the two peaks of a cyclic stress. The consequences of the model will have significant bearing on our ultimate concern, which is the attenuation of stress waves. We assume that the evolution of slip in the plastic zone, via the mechanism of slip banding, cannot be an instantaneous process, but is rather one that takes place with a time constant that implies some sort of rate process. Let us call this time-dependent process of evolution a creep viscosity, where the term "viscosity" is intended to describe the fact that the slip bands and the other microscopic manifestations of plasticity cannot form instantaneously, but instead they form and slip along them takes place over some extended time interval. In some sense, this time constant could be measured by applying a stress greater than the yield stress to the plastic zone, and measuring the rate at which it deforms. Whether this "viscosity" is characteristic of a linear or a non-linear process is probably not too important for our purposes here; a method for its identification will be noted below.

Within the plastic zone, there is a gradient of yield strength ranging from zero at the crack tip. up to the material yield strength at the elastic-plastic zone boundary; we call this the local yield strength. The precise form of this distribution depends on the nature of the slip-weakening physics but the details are probably not too

important for this discussion. The local yield strength is evidently determined by the peak applied stress, and can be obtained by interpolation between zero, the value at the crack tip and σ_Y at the plastic zone boundary at distance R.

If there is a time constant for the development of slip, then slip must continue to take place over at least part of the plastic zone, during the times when the stresses are positive, including the waning portion of the sinusoidal stress cycle. These stresses continue to cause creep motions in part of the plastic zone even though the stress is not at the maximum. As the excitation stresses decrease after reaching the peak, the stresses will be at the local yield strength in a smaller and smaller part of the plastic zone, more and more concentrated near the crack tip; this zone contracts from the largest dimension of the plastic zone reached when the load or external stress is at its peak. In the inner, contracting zone, (Fig. 4), creep on slip bands continues to take place, while on the outer parts of the plastic zone bubble, slip will have ceased, and this outer part of the plastic zone now responds only elastically. Continued displacement due to creep in the contracting plastic zone will generate an increase in the "damage", i.e. a lowering of the local strength in the region near the crack tip, when compared with the condition at the peak.

As the applied stress increases on the next cycle, the accumulated damage (to use Weertman's term) near the crack tip is higher than that at the time of the preceding maximum and the local strength is lower; and thus the crack advances. The crack advances because the stress
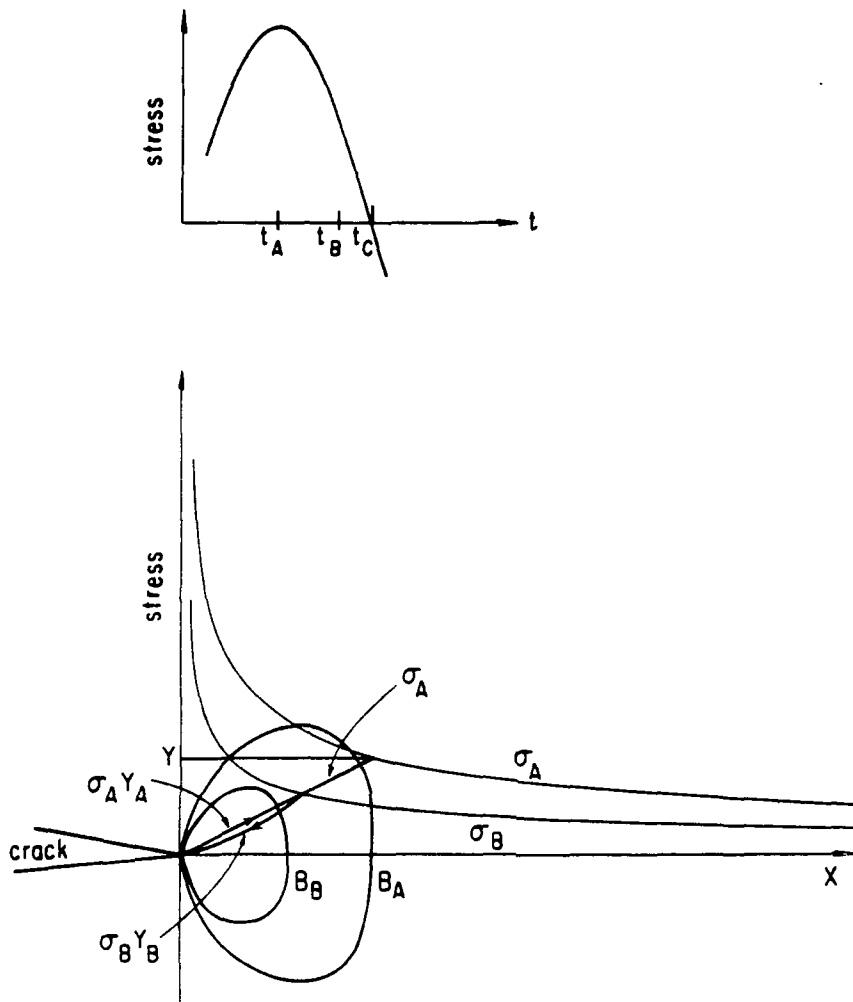
Figure 4. Schematic diagram illustrating collapse of the plastic zone "bubble" upon unloading. At time of maximum stress t_A, the plastic zone has a boundary B_A; the stress distribution is given by σ_A; inside the plastic zone, the yield strength is equal to the stress σ_A.

At time t_B, the plastic zone bubble of active creep has collapsed to boundary B_B. The region between B_A and B_B remains damaged but damage is not increasing due to active creep at time t_B. Continued creep with B_A reduces the strength to below the value it had a time t_A. At t_B the stress distribution is σ_B.

profile gives a stress in the neighborhood of the crack tip that is greater than the strength of the plastic zone, as a consequence of the earlier accumulated creep near the crack tip. The crack advances by an amount so that the stress profile for the increasing stress and the local strength profiles are tangent, most of the creep damage on the waning stress cycle is localized near the crack tip, where the material remains plastic even under small stress. Thus the advance of the crack tip takes place early in the episode of increasing stress. But the outer elastic-plastic boundary only advances when the stress is near the maximum. Thus the inner parts of the plastic zone undergo increased creep in the early stages of an increasing later cycle of applied stress; as the stress increases, the zone of increased creep progressively moves outward in the plastic zone. When the sinusoidal stress is near the maximum, the creep "wave" encounters the old elastic-plastic boundary, and only then does the boundary move outward. To summarize, the crack tip advances in the early stages of the increasing stress on the next cycle and the elastic-plastic boundary moves outward when the applied stress is close to the maximum of the cycle. We return to the latter point when we design an algorithm to calculate the response to an oscillatory wave packet in the time domain.

The introduction of the concept of continued creep in the damaged region means that the rate of deformation will depend on a rate of formation of deformation such as slip banding in the plastic region. Thus the amount of slip will be dependent on the time interval over which the stress remains positive (see interval t_A to t_C in Fig. 4).

-22-

It follows that the amount of crack growth will be a function of the frequency of the applied load stress. Hence the experimentally determined rate of crack growth should show a significant decrease with increasing frequency of the external applied stress, a prediction consistent with the experimental results of James (1972) (Fig. 5). In principle, the frequency dependence in these experiments should provide a method of determining some features of the creep viscosity in the plastic zone. As remarked, we do not expect that the viscosity should depend significantly on the constitutive law profile for the strength distribution in the plastic zone; Chen and Knopoff (1986a) have shown that two relatively remote constitutive laws for the slip-weakening zone lead to approximately similar stress profiles in the plastic zone. We return shortly to the question of the dependence of the deformation on the amplitude of the applied stress.

This model allows us to understand the physical reasons behind several of the experiments performed with time-dependent loading. Spectrum loading is itself a subject for experimental investigation that has commanded an extensive literature (see Wheeler, 1972; von Euw, et al., 1972; Wei and Stephens, 1975; Kogaev and Lebedinskii, 1985, for example). In the spectrum loading problem, an amplitude modulation of the sinusoidal excitation is applied to the material; often the amplitude modulation is restricted to a single cycle having an unusually large peak amplitude, with the remainder of the time series being a cyclic excitation of relatively constant amplitude (Fig. 6). In general, the experimental results show that the crack growth rate reaches a plateau for an extended time following the application of the

STRESS INTENSITY FACTOR RANGE ΔK, kg/(mm)$^{3/2}$
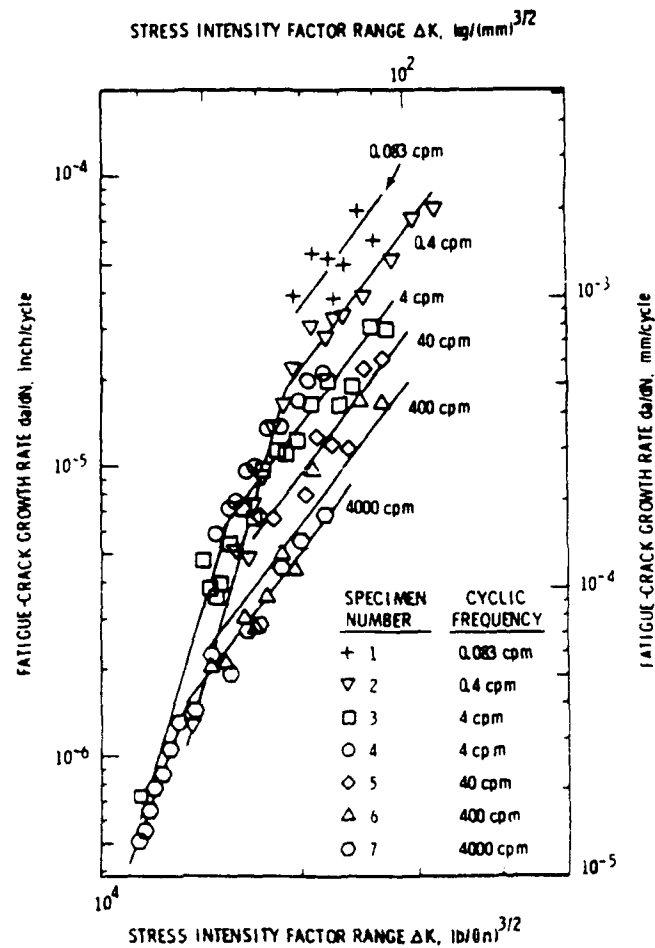
-The effect of frequency on the crack growth behavior of solution-annealed
Type 304 stainless steel at 1000 F.
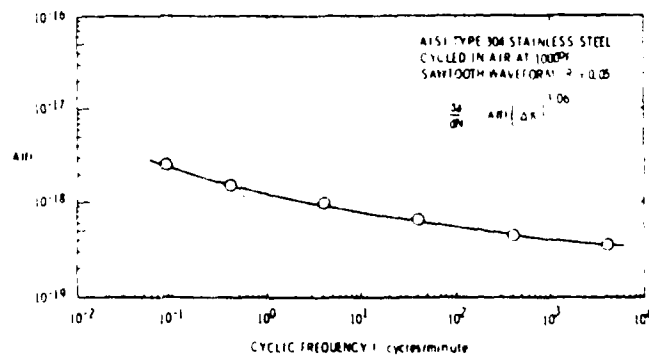
-Design curve for the effect of cyclic frequency on Type 304 stainless
steel at 1000 F.

Figure 5. Effect of frequency crack growth in stainless steel. The crack growth
rate is lower for higher frequencies of loading. (Data taken from James, 1972).

-24-
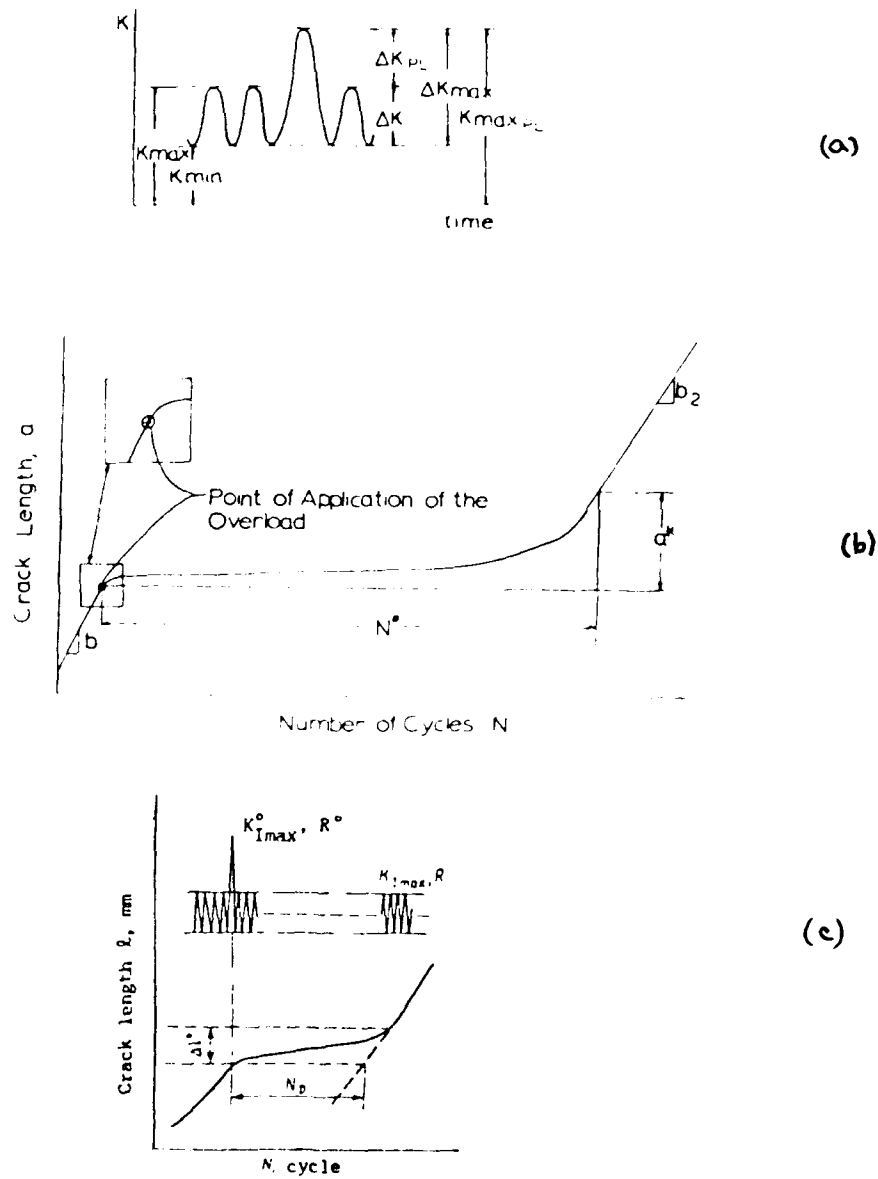
Figure 6. Schematic diagram of spectrum loading with sinusoidal load stress, showing reduction in growth rate after application of a singular spike. (Diagrams (a,b) from von Euw, et al. (1972); (c) from Kogaev and Lebedinskii (1985).

extraordinary large stress; after some time, growth resumes. The result can be understood in terms of the above model as follows (see Fig. 7): At the time at which the applied stress is at its greatest peak, the strength profile in the plastic zone is given by the same construction as before; the plastic zone will have grown dramatically compared with growth rates just before the spike. During the episode of waning stress in the wake of the extraordinary peak, the strength in the region near the crack tip is significantly lowered due to post-big-peak creep. On the increase of stress leading to the next "normal" peak, the stress profile follows the strength profile that has been left in the wake of the extraordinary peak, the strength in the part of the plastic zone nearest the crack tip can no longer support stresses of that magnitude; the stresses in the remainder of the plastic zone are less than the strength. The stress due to the lesser peaks is indeed small, but nevertheless the stress in a small part of the plastic zone is greater than the local strength; the strength curve that has been set up by the waning branch of the extraordinary stress pulse is concave upwards relative to the constitutive relation, the latter is drawn in Fig. 7 as a straight line. The excess of stress over the strength is only a small amount, so that the crack now advances very slightly, and continues to do so for a long sequence of "normal" oscillations. The crack tip advances to a position so that the stress curve now lies outside the concave strength curve. During all of this plateau period, the outer plastic-elastic boundary remains more or less fixed in the position it had at the time of the extraordinary peak. After many cycles after the spike, the more rapidly moving crack tip at last approaches the slower moving plastic
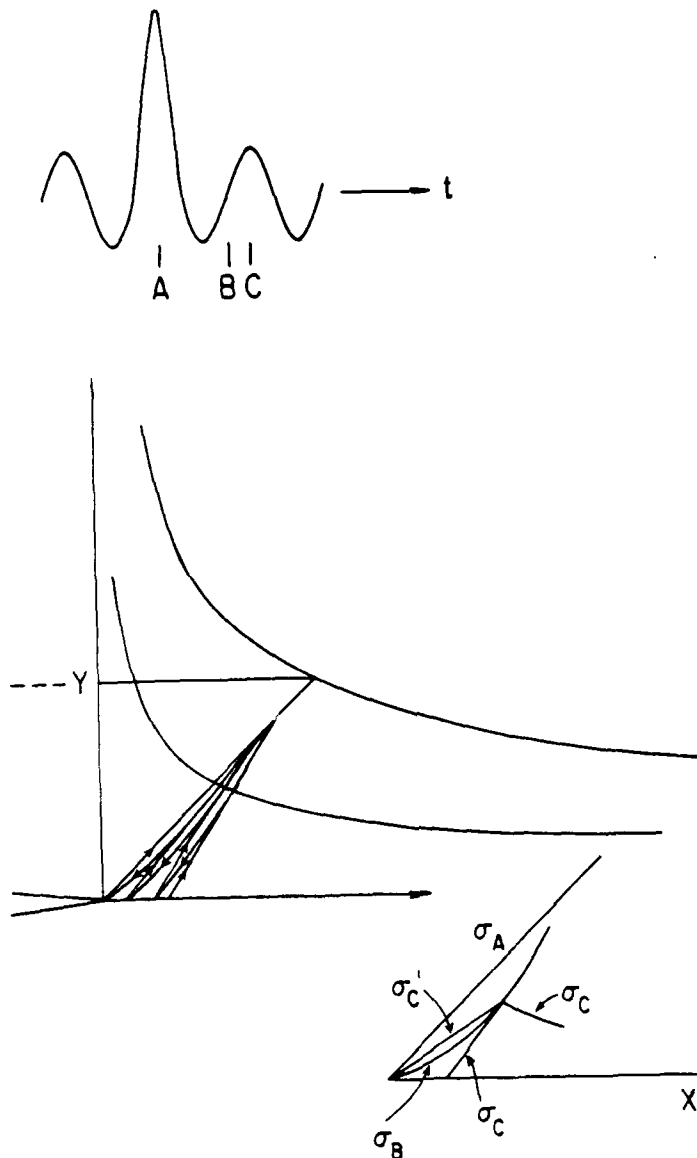
Figure 7. An extraordinary peak in a spectrum loading experiment causes a large plastic region to appear. Due to accumulated creep damage near the crack tip, the strength profile is concave upward. The stress profile on a subsequent smaller peak is greater than the concave strength profile and the crack tip advances slightly; the plastic zone boundary remains fixed.

As a peak t_A, the stress/strength profile in the plastic zone is σ_A. At time of zero crossing t_B, the stress ahead of the crack is zero and the strength is given by the curve σ_B, which is lower than σ_A because of the accumulated creep damage between the two times. At time t_C, the calculated stress in the plastic zone σ_C' is greater than the strength σ_B; the crack tip then advances a small amount and the new stress profile both inside and outside the plastic zone is σ_C. The central diagram illustrates the advance of the crack after several cycles of reduced stress peaks in the shadow of the extraordinary peak.

zone boundary, the strength profile now becomes a relatively steep one, the size of the plastic zone is again relatively small, creep decay is now relatively large once again, and the crack resumes its growth at the "normal" rate.

IV. An Approximate Model

The application of the model of accumulated damage to the problem of attenuation of stress waves that are non-sinusoidal but nevertheless oscillatory is difficult. We must convolve the accumulated creep with the complete stress-time history. The development of a computational model to accomplish this task is being undertaken at the present time. Pending this development, we offer a simple and hopefully adequate-in-some-respects algorithm that simulates some of the features of the above crack growth model. The approximate model works well for sinusoidal excitations and may work well for non-sinusoidal stresses that are relatively non-drastic perturbations of sine waves.

Most of the stress wave energy loss and hence attenuation is associated with the outward motion of the elastic-plastic boundary. Thus stress wave attenuation is associated with the peaks of the loading cycle for those peaks that are about as large or larger than their predecessors. The amount of motion depends on the cumulative damage in the interval since last motion of the boundary. which we estimate by the time over which the stress has been applied. We use the following empirical procedure for implementing these ideas. From a

stress maximum, draw an exponentially decaying curve with some given time constant, which is a parameter of the system. At the point of intersection of this decay curve with a rising curve of stress excitation, we identify the base stress level from which growth of the plastic zone boundary takes place. A new exponential decay curve is started from the next maximum in the stress excitation function (Fig. 8). If an exponential decay curve skips over the top of a subsequent crest and strikes a later rising curve of stress, then the intervening stress cycles are ignored and energy loss is calculated from the new point of intersection. To ensure universality, i.e. to be able to apply this rule to a wide variety of materials, we require that either the decay rate be very small or very large. It cannot be very large at acoustic frequencies, since this would generate an intersection at every zero crossing (in an increasing sense) of the stress wave function, which is the Paris model and we have argued that this model is inappropriate. Thus the exponential decay rate is probably small.

To calculate the Q for _harmonic_ _excitation_ under the conditions of this model of damage, we proceed as before, with the exception that the energy lost per cycle is now proportional to the amount of new material converted to the plastic or slip-weakened state. The area of advance of the slip-weakening zone bubble on any cycle is the area of a crescent-shaped (lune) region at the outer edge; the area of the lune is proportional to the quantity $(L \cdot dL)$ where L is the radius of the plastic zone and dL is the amount of growth per cycle. As before, $L \sim K^2$; in this case, the displacement of the plastic zone boundary is
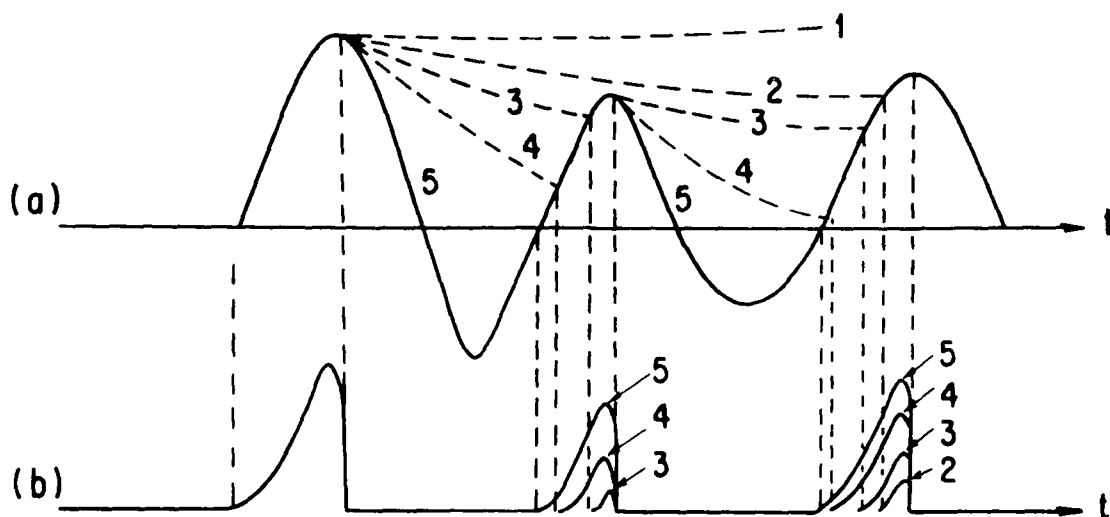
Figure 8. Schematic diagram to indicate effects of creep on
attenuation in cases of fatigue crack growth.

- a) Hypothetical Oscillatory Stress Excitation (solid) with various
  presumed decays to simulate effects of creep in plastic zone
  during waning part of oscillatory stress.
  1) Creep time constant $\tau = \infty$.
  2) Large creep time constant so that exponential decay fails to
     intersect a weaker stress pulse occurring later.
  3,4) Smaller creep time constants, creating intersections with
     the flanks of a later, weaker stress oscillation.
  5) Creep time constant $\tau = 0$; $K^* = 0$.
- b) Non-transmitted (absorbed) stress.

equal to the amount of growth of the crack at its tip. The latter quantity is proportional to the damage in the vicinity of the crack tip. From the Paris Law, the incremental growth per cycle must be proportional to $K^3 \Delta K_r$, where ΔK_r is the amount of stress relaxation due to creep in the plastic zone in the interval between stress peaks. The quantity ΔK_r depends only on the the viscous creep rate and the time between peaks of the sine wave and is independent of the external stress; ΔK_r cannot depend on the external stress, since the interior of the plastic zone is already at the critical state. Thus the increase in area, and as a consequence the energy lost per cycle, is proportional to K^5. Since the peak energy is proportional to K^2, it follows that Q^{-1} for harmonic excitation for this model must vary as the third power of the stress, i.e. with the same exponent as in the velocity of growth law. It is of interest to note that the third power law for growth of cracks, which must correspond to the creep deformation rate in the plastic zone, is approximately the same exponent that is appropriate for the nonlinear viscosity of the lower crust and upper mantle under excitation rates that are orders of magnitude slower than those in the laboratory experiments of fatigue crack growth, but this may only be coincidental. Our prediction that the growth rate per cycle is $K^3 \Delta K_r$, with ΔK_r independent of the stress, and hence is proportional to the third power of the applied stress, is confirmed experimentally (James, 1972).

To summarize the approximate model, we have assumed that K^* on any increasing stress cycle is a monotonically decreasing function with elapsed time since an earlier stress peak; we propose that this creep

decay time be a constant of the system. In figure 8, an application of

a first episode of increasing stress produces absorption (of stress)

proportional to the quantity $K^3(dK/dt)$, where K is itself proportional

to the stress. This follows directly from the ordinary formula (2) for

application of a monotonic stress to fresh material. With regard to

the response in the oscillatory part of the excitation history, a creep

decay with infinite time constant such as curve 1, produces a temporal

shadow on later cycles of the oscillatory stress wave so that there

will be no absorption. An exponential decay curve such as curve 4,

will intersect a later oscillatory stress at some point along its flank

and trigger crack growth (and hence absorption) from this point; the

intersection of the exponential decay and the increasing stress curves

identifies the value of K^*. In the case of a zero decay constant

(curve 5), the value of K^* is zero. (For the purposes of illustration,

we have assumed that crack growth only takes place on the increasing

part of the positive half cycle of stress. As remarked, more properly,

growth for shear cracks will take place on both the positive and

negative half cycles of increasing absolute stress.) For purely

sinusoidal excitation (with constant amplitude), the energy lost per

cycle in this model depends on the ratio between the creep decay times

in the plastic zone and the period of the applied stress. There are

two extreme models. For large decay rates (or extremely long periods),

Q will be independent of frequency; for small creep decay rates (which

corresponds to high-frequency experiments) and for linear creep in the

plastic zone, the approximate model suggests that Q^{-1} will vary as ω^1.

The proof of the later statement is simple: for small relaxed stresses

in the plastic zone, the stress relaxation ΔK_1 will be of the order of

ηT at the time of the next peak of stress, where η is a creep rate and T is the period. Thus the energy loss per cycle will be proportional to ω^{-1}.

V. Crack-Growth due to Stress Corrosion

In the stress-corrosion case, it is found experimentally that

$$v = dL/dt \sim e^{K/K_o} \quad \text{or} \quad v \sim K^n \tag{3}$$

where n is a large number. Values of n range from 10 to 170 (Atkinson, 1982, 1984; Swanson, 1984). The exponential and power law versions fit the data about equally well over the range of stress intensity factors in most experiments; the exponential version has a physical basis in thermodynamics. The quantity K_o is proportional to temperature and thus stress corrosion can be identified with a thermal activation process. The physics of the process is not that of bond breaking by the application of excess stress, as it is in the fatigue crack cases, but instead works by chemical or hydrolytic bond weakening of the silicon-oxygen bond in silicates, due to the action of the fluid. This too is a time dependent process; the number of bonds that break depend on how long the excess stress has been applied. Once again a slip-weakening zone develops with the greatest damage being found near the crack tip. If the rate at which silicate bonds can be attacked is very slow compared to the stress (sinusoidal) excitation rates, Q will be frequency dependent as for fatigue cracks, with exponents that will depend on the rate of deformation in the plastic zone; as above, Q will

vary as ω^1 for small relaxations; the higher Q's correspond to the shorter times available for the stress to act in the cases of high frequency excitation. For rapid reaction rates, Q will be independent of the frequency, but this is probably unlikely to be the case at seismic frequencies. If the energy needed to break bonds is small, the energy in the seismic wave will be dissipated in the migration of the plastic zone, but if the energy for bond breaking is not insignificant, Q^{-1} will have an additional term in the stress dependence. By the argument given above for fatigue cracking, Q^{-1} must vary as σ^3.

In both the fatigue crack and stress corrosion cases, there is a plastic zone in the neighborhood of the crack tip. The function of the corrosive fluid is to weaken the bonds at the crack tip; this therefore plays the same role as the bond-weakening creep that has been described for fatigue cracking. Thus the attenuation response mechanism is the same in both cases. There is however a competition between the two processes: the one with the faster rate will dominate the rate at which the bonds are weakened. From eq. (4), stress corrosion effects will dominate at large stress intensity factors. The stress and frequency dependence of Q^{-1} in the stress corrosion case are likely to be the same as in the fatigue cracking case, as long as the creep is small between successive peaks of an oscillatory stress. The increased creep "viscosity" at high stress intensity factors means that the transition between the small damping and the large damping regime is found at higher frequencies; in this case, as remarked, Q would be likely to be frequency independent over a broader (low-)frequency range.

-34-

Both the stress corrosion and fatigue cracking mechanisms are generic. We can generalize by noting that any Markov process for which the work done in energy removal from the deformation is dependent only on the state of stress on the system at the time will yield a value of Q that is likely to depend on an even power of the frequency, while non-Markovian processes such as energy loss by frictional forces that depend on velocity, i.e. such that the work done depends on how long the forces have been applied, are likely to give odd powers of the frequency exponent for Q (Knopoff, 1964). Both the cases of extension due to fatigue cracking and stress corrosion are examples of attenuation with time-delay effects, and must therefore be considered to be non-Markovian processes.

VI. Non-sinusoidal Excitation

We have considered the attenuation due to these nonlinear mechanisms for cases of excitation wave forms that simulate first, stress waves due to explosions and second, seismic signals considered by engineers to be appropriate to describe ground motion in large earthquakes. Our simulations were straightforward; in the explosion example, we used a simple pulse from SALMON. The attenuation waveform in both cases was computed by generating the function $\sigma^3(d\sigma/dt)$ from the stress wave. In the explosion case we assumed that this operated only on the waxing part of the stress waveform. In the seismic ground motion case we used the approximate model with three different values of the decay exponent that is designed to simulate creep during the

unloading or waning portion of the stress cycle (not important for the case of the simple pulses from explosions). According to the approximate model of Fig. 8, we then applied the above operator on the waxing part of the stress wave for stresses greater than the intersection of the decay curve from the preceding peak.

Although it is not permissible to take the Fourier transform of a non-linear operator, we can easily find the equivalent transfer function of the operator, by comparing the spectra of the excitation and absorbed signals. The fit of the dependence of Q on frequency has been obtained by a maximum-likelihood estimation technique, assuming a power-law dependence of Q on the frequency. In both cases, whether for explosion (Fig. 9) or earthquake ground motion waveforms (Fig. 10), we find that $Q \sim \omega^1$, in unexpected agreement with the theory for sinusoidal excitation (Table 1).

In fact, examination of Table 1 shows that the exponent is somewhat less than one in varying amounts that depend on the decay constant. Below we present arguments that the Q^{-1} spectrum should have a curvature that depends on a characteristic time or frequency for the seismic signal. Since in this case the characteristic frequency is the corner frequency, we expect, from qualitative arguments given in the next section that the estimates of slope of the log Q^{-1} vs. log frequency curve are contaminated by source spectrum effects and that neither of the curves of Figs. 9 and 10 are independent estimates. But the slope at frequencies less than 1.5 hz, i.e. at the low frequency end of Fig. 10 is a more reliable estimator of the exponent.
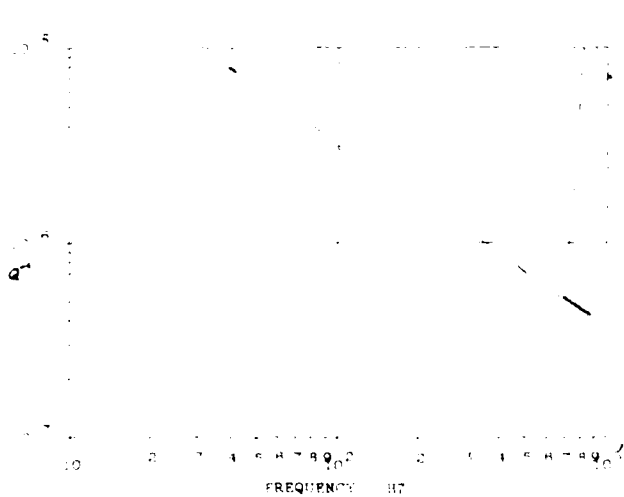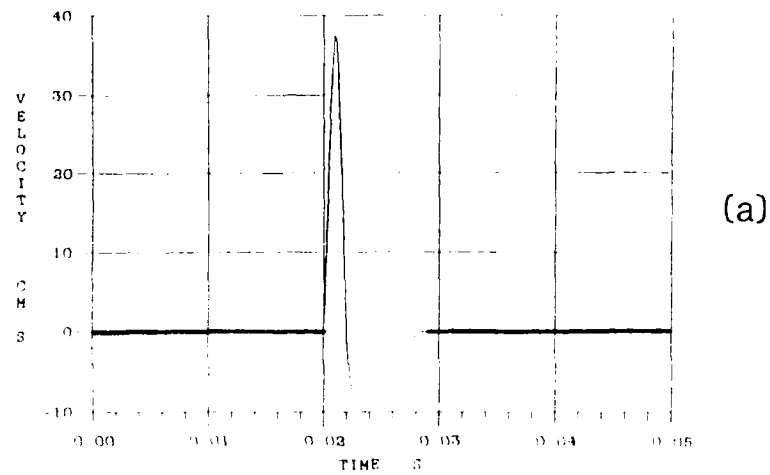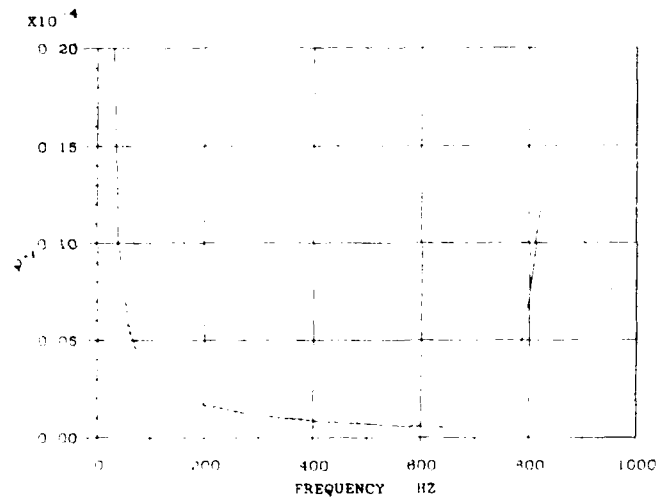
Figure 9. a) Stress wave from nuclear event SALMON (after McCartor and Wortman, 1985). b) log Q^{-1} as a function of log frequency for fatigue crack growth model for SALMON record. Interrupted solid line is power law fit with exponents given in Table 1. Note rise in Q^{-1} at extreme right-hand end of diagram corresponding to effect of finite pulse duration. c) Same as b) with linear Q^{-1} vs frequency plot.
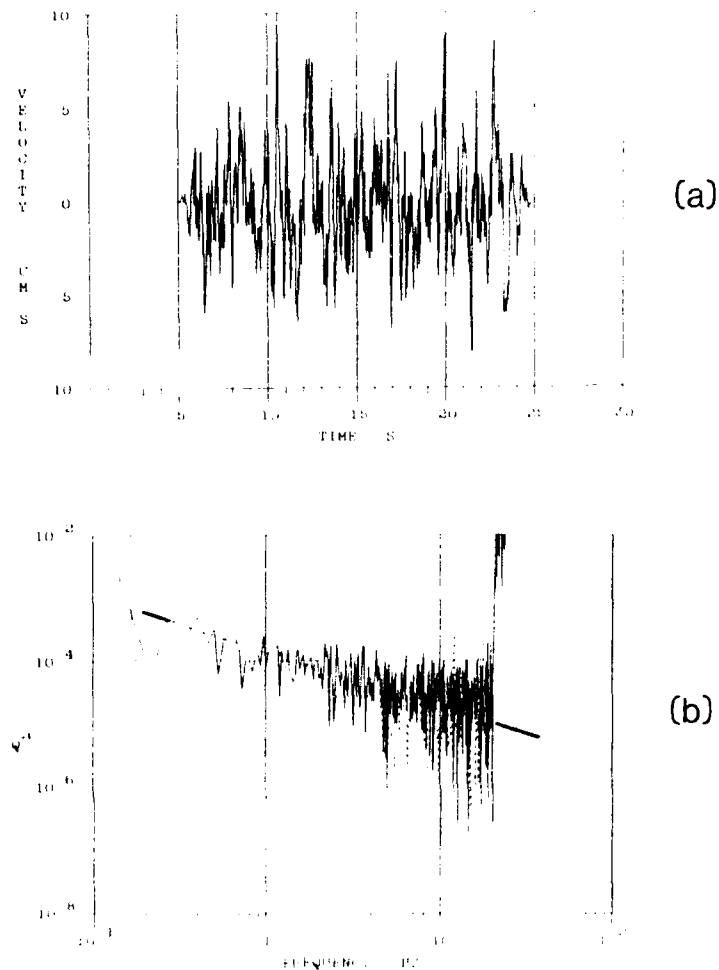
Figure 10. a) Stress wave for simulated strong earthquake ground motion. Displacement spectrum has corner at 1.5 hz with ω^{-1} rolloff; bandwidth extends from 0.05 hz to 20 hz. The phases are random. (Program after Gasparini and Vanmarcke, 1976.) The ω^{-1} rolloff is inconsistent with the more commonly accepted ω^{-2} model (Brune, 1970) which is a theory for small earthquakes. Haskell (1964) suggested that ω^{-1} might be more appropriate for large earthquakes, because of "stuttering" during rupture. Actual exponents for large earthquakes fall between these two values (see Hartzell and Heaton, 1985, 1988, for example.) b) $\log Q^{-1}$ vs. log frequency for fatigue crack growth model. Interrupted solid line is power law fit with exponent given Table 1. Creep decay constant is zero.

Table 1

Maximum likelihood estimates of exponent α

Power Law Fit $Q^{-1} = Af^{\alpha}$ to Spectral Analyses

| | decay times τ (sec) | | |
	$\tau = 0$	$\tau = 0.4$	$\tau = \infty$
Earthquake Ground Motion	-0.923	-0.841	-0.776[*]
Explosion	-0.956		

[*]The exponent approaches -1 if the bandwidth is narrowed to include only frequency estimates below the corner frequency.

Numerical experiments with the diagram of Fig. 10 show that this is indeed the case with the slope steepening appreciably toward -1 as one uses a smaller and smaller sample of frequencies, biased toward the low-frequency end of the spectrum. This issue is discussed in the next section, with reference to the results shown in Fig. 9.

We can make the obvious argument for the differences between the results for harmonic excitation, with zero exponent at extremely low frequencies and with an exponent of -1 in the case $\tau = 0$. We suppose that this is due to the frequency multiplication by the non-linear operator, and the feedback at irregular phase of significant amounts of multiples of the low frequency parts of the signal into the higher frequency parts of the spectrum. In the case of sinusoidal excitation, the scattered signal never reappears as higher harmonics in the detection pass band of the system for a narrow band-pass detector. We note that the case $\tau = 0$ which gave an result of 0 independent of frequency in the sinusoidal case, gave the exponent closest to unity in the case of the simulated seismic ground motion.

VII. Simple Model of an Explosion Waveform

We can derive an approximate expression for $Q(\omega)$ in the case of crack-growth absorption for the problem of excitation by an explosion signal. For small attenuation we can write

$$\frac{\omega}{Q} \sim \frac{\text{F.T.(absorbed signal)}}{\text{F.T.(incident signal)}}$$

Let us represent the main part of the excitation from the explosion as a distorted half-cycle of a sine wave (Fig. 11). Since the K^3 operator is significant only near the peak, the absorbed signal will be essentially a short pulse of some width τ. The Fourier transform of the absorbed signal will be essentially of the form appropriate to a pulse of duration τ, namely proportional to $\sin(\omega\tau)/\omega$. The Fourier transform of the incident signal will be essentially proportional to a function having the form $\sin(k\omega T)/\omega$, at least for low frequencies; the details of the spectrum will depend on the particulars of the wave shape, but for this rough calculation, our description will suffice. The time T is the interval between the first arrival and the first zero crossing of the incident wave function. We gauge the size of the coefficient k by the frequency of the first zero crossing of the spectrum. For a square wave (incident pulse), the first zero crossing is at $1/T$ (and the spectrum above is exact): hence $k=1$. For a half-cycle of a sine wave, the first zero crossing is at $3/2T$; we set $k=2/3$. (For a delta function, the first zero crossing is at ∞/T.) Thus
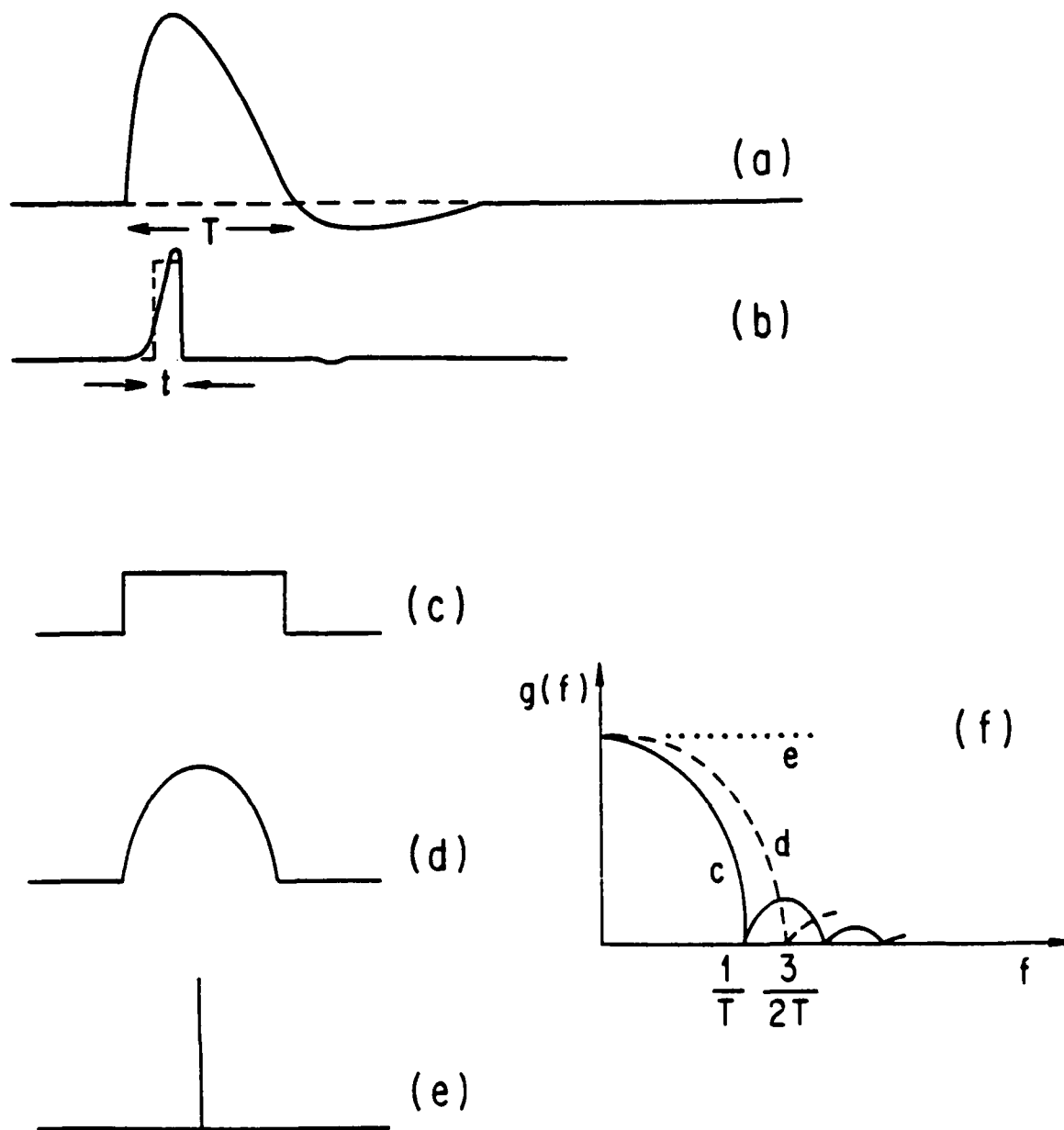
Figure 11. a) Schematic explosion stress pulse. The first large oscillation has a duration $\underline{T}$. b) Schematic non-transmitted (absorbed) part of stress signal due to fatigue crack growth (solid). The absorption signal is concentrated near the peak of the first large oscillation in the incident signal. We represent the absorption signal by a square wave of duration τ. c) Square wave representation of the incident impulse. d) Half-cycle sine wave representation of the incident impulse. e) Delta function representation of the incident impulse. f) Spectra of the three approximate representations of the incident impulse. The first zero in the spectrum of a) is near 1.8/T.

the more spiky the first pulse, the larger the value of k. Thus the spectral behavior of Q^{-1} is approximately

$$Q^{-1} = \omega^{-1} \frac{\sin(\omega\tau)/\omega}{\sin(k\omega T)/\omega}$$

$$= \omega^{-1} \frac{\sin(\omega\tau)}{\sin(k\omega T)}$$

Thus, at low frequencies, $Q^{-1} \sim \omega^{-1}$. There should be a peak in the spectrum of Q^{-1} at the frequency corresponding to the first minimum in the spectrum of the incident pulse. Since the first half-cycle of the incident pulse has a duration of about 0.002 sec, and since the incident pulse is slightly more spiky than a half cycle of a sine wave, it follows that a peak in the Q^{-1} spectrum at about 900 hz is not unreasonable (k=1.8) which suggests a slightly more spiky waveform than a half-cycle sine-wave; there is indeed a minimum in (our) spectrum of the SALMON recording at the correct value. The use of spectra to study Q^{-1} unfortunately leads to expected and not very revealing results: Q^{-1} should vary as ω^{-1} for any pulse, independent of the mechanism; the first peak in the spectrum only gives information about the spectrum of the exciting signal. Neither property gives information about the mechanism of absorption. Thus we are obliged to discard spectral analysis as a possible means of identifying absorption mechanism. To identify mechanism, we must analyze the waveforms in the time domain in these strongly nonlinear circumstances. This means that the analysis of attenuation on real signals must also be done in the time domain;

frequency analysis is likely to yield little information on this problem.

VIII. Conclusions

1) It is possible to understand the behavior of absorption for harmonic excitations for reasonable, though non-linear, physical mechanisms; in this discussion we have considered absorption due to fatigue crack growth and stress corrosion.

2) At large strains, the fatigue crack process is not independent of creep effects. To explain the results of amplitude modulated sinusoidal excitations, or spectrum loading as it is called in the engineering literature, we have been obliged to introduce creep in the slip-weakening or plastic zone near the crack tips. Deformation continues to take place in this zone even though the stress may be in the waning part of any cycle. This process allows for continued crack growth on later cycles of applied stress, even though the crack would have appeared to reach the length appropriate to the maximum of the cyclic stress. Both stress corrosion cracking and fatigue cracking turn out to be non-Markovian in nature and hence to have frequency dependent Q's at frequencies of excitation that are large compared with the relaxation frequency.

3) Under fatigue crack conditions, $1/Q$ varies as the cube of the harmonic excitation amplitude.

4) Because of the non-linearity, one should not expect the results from sinusoidal excitation and non-sinusoidal (including impulsive) excitation to agree. In the cases of fatigue crack growth and stress corrosion, both non-linear mechanisms, Q is frequency independent for a purely sinusoidal excitation, and detection by a narrow bandwidth detector; for an impulsive or broad band seismic signal with broadband detection, $Q \sim \omega^{-1}$.

5) For non-time harmonic excitation, it is possible to derive a transfer function for the non-linear attenuation operator. For widely divergent excitation waveforms, Q varies approximately as ω^1. Unfortunately, this result is probably due to the fact that the absorption mechanism operates over a short time interval during the stress cycle. Hence spectral analysis is likely to give very little information about the nature of the absorption mechanism. Recourse should be made to analysis in the time domain. To study the mechanism, we must analyze the waveforms in the time domain in these strongly nonlinear circumstances. This means that the analysis of attenuation on real signals must also be done in the time domain; frequency analysis is likely to yield little information on this problem.

REFERENCES

D.L. Anderson, H. Kanamori, R.S. Hart and H.P. Liu, The Earth as a Seismic Absorption Band, Science, 196, 1104-1106, 1976.

D.J. Andrews, Rupture propagation with finite stress in antiplane strain, J. Geophys. Res., 81, 3575-3582, 1976.

B.K. Atkinson, Subcritical crack propagation in rocks: Theory, experimental results and applications, J. Struct. Geol., 4, 41-56, 1982.

B.K. Atkinson, Subcritical crack growth in geological materials, J. Geophys. Res., 89, 4077-4114, 1984.

G.I. Barenblatt, The Mathematical Theory of Equilibrium Cracks in Brittle Fracture, Advances in Applied Mathematics, 7, 55-129, 1962.

J.N. Brune, Tectonic Stress and the Spectra of Seismic Shear Waves from Earthquakes, J. Geophys. Res., 75, 4997-5009, 1970.

Y.T. Chen and L. Knopoff, Static Shear Crack with a Zone of Slip-Weakening, Geophys. J. Roy. Astron. Soc., 87, 1005-1024, 1986a.

Y.T. Chen and L. Knopoff, The Quasistatic Extension of a Shear Crack in a Viscoelastic Medium, Geophys. J. Roy. Astron. Soc., 87, 1025-1039, 1986b.

G.P. Cherepanov, Mechanics of Brittle Fracture, McGraw-Hill Book Co., New York, 1979.

D.A. Gasparini and E.H. Vanmarcke, Simulated Earthquake Motions Compatible with Prescribed Response Spectra, NSF Grant ATA 74-06935, Report No. 2. Available as U.S. Department of Commerce NTIS Report MIT CE R76-4, Jan. 1976.

D.T. Griggs, Bull. Geol. Soc. Amer., Experimental Flow of Rocks under Conditions Favoring Recrystallization, 51, 1001-1002, 1940.

D.T. Griggs and J. Handin, Observations on fracture and a hypothesis of earthquakes, Geol. Soc. Amer. Mem., 79, 347-364, 1960.

J.C. Grosskreutz, Fatigue Mechanisms in the Sub-Creep Range, in Metal Fatigue Damage-Mechanism, Detection, Avoidance and Repair, Amer. Soc. Testing Materials, Spec. Tech. Publ. 495, 1971, pp. 5-60.

S.H. Hartzell and T.H. Heaton, Teleseismic Time Functions for Large, Shallow Subduction Zone Earthquakes, Bull. Seismol. Soc. Amer., 75, 965-1004, 1985.

S.H. Hartzell and T.H. Heaton, Failure of Self-Similarity for Large (M_w>8-1/4) Earthquakes, Bull. Seismol. Soc. Amer., 78, 478-488, 1988.

N.A. Haskell, Total energy and energy spectral density of elastic wave radiation from propagating faults, Bull. Seismol. Soc. Amer., 54, 1811-1841, 1964.

R.G. Hoagland, G.T. Hahn and A.R. Rosenfeld, Influence of Microstructure on Fracture Propagation in Rock, Rock Mechanics, 5, 77-106, 1973.

J.A. Hudson, A higher-order approximation to the wave propagation constants for a cracked solid, Geophys. J. Roy. Astron. Soc., 87, 265-274, 1986.

J.A. Hudson and L. Knopoff, Predicting the overall properties of composites- materials with small-scale inclusions or cracks, PAGEOPH, Special Volume, edited by R. S. Wu and K. Aki, In Press, 1989.

Y. Ida, Cohesive force across the tip of a longitudinal shear crack and Griffith's specific source energy, J. Geophys. Res., 77, 3796-3805, 1972.

L.A. James, The Effect of Frequency upon the Fatigue-Crack Growth of Type 304 Stainless Steel at 1000 F, Stress Analysis and Growth of Cracks, Amer. Soc. Testing Materials, Spec. Tech. Publ. 513, 1972, pp. 218-229.

L. Knopoff, Q, Revs. of Geophysics, 2, 625-660, 1964,

L. Knopoff and G.J.F. MacDonald, Attenuation of Small Amplitude Stress Waves in Solids, Revs. Mod. Phys., 30, 1178-1192, 1956.

L. Knopoff and G.J.F. MacDonald, Models for acoustic loss in solids, J. Geophys. Res., 65, 2191-2197, 1960.

V.P. Kogaev and S.G. Lebedinskii, Propagation of Fatigue Cracks in the Region of the Effect of Overload, Problemy Prochnosti, pp. 35-41, Nov. 1985 (English Translation).

B.V. Kostrov and S. Das, Idealized Models of Fault Behavior Prior to Dynamic Rupture, Bull. Seismol. Soc. Amer., 72, 679-703, 1982.

T.H. Lin, Micromechanics of Deformation of Slip Bands under Monotonic and Cyclic Loading, Reviews on the Deformation Behavior of Materials, 2, 263-316, 1977.

G.D. McCartor and W.R. Wortman, Final Report: Experimental and Analytic Characterization of Nonlinear Seismic Attenuation, 20 March 1985, AFOSR Contract #F49620-84-C-0049.

B. McKavanagh and F.D. Stacey, Mechanical Hysteresis in Rocks at Low Strain Amplitudes and Seismic Frequencies, Physics Earth Planet. Interiors, 8, 246-250, 1974.

J.B. Minster, Anelasticity and Attenuation, in Fisica dell'Interno della Terra, Proc. Enrico Fermi International School of Physics, Course 78 (A.M. Dziewonski and E. Boschi, eds.), pp. 152-212, 1980.

J.B. Minster and D.L. Anderson, Dislocations and Nonelastic Processes in the Mantle, J. Geophys. Res., 85, 6347-6352, 1980.

A.C. Palmer and J.R. Rice, The Growth of Slip Surfaces in the Progressive Failure of Overconsolidated Clay, Proc. Roy. Soc., A332, 527-549, 1973.

P.C. Paris, The Fracture Mechanics Approach to Fatigue, Chapter VI, of Fatigue- an Interdisciplinary Approach, (J.J. Burke, N.L. Reed and V. Weiss, eds.,) Syracuse Univ. Press, 1964, pp. 107-132.

J.R. Rice, Mechanics of Crack Tip Deformation and Extension by Fatigue, Fatigue Crack Propagation, Amer. Soc. Testing Materials, Special Tech. Publication 415, 1967.

J.R. Rice, The Mechanics of Earthquake Rupture, in Physics of the Earth's Interior, pp. 555-649, eds. A.M. Dziewonski and E. Boschi, North Holland Publ. Co., 1980.

F.D. Stacey, M.T. Gladwin, B. McKavanagh, A.T. Linde and L.M. Hastie, Anelastic Damping of Acoustic and Seismic Pulses, Geophys. Surveys, 2, 133-151, 1975.

P.L. Swanson, Subcritical Crack Growth and other Time- and Environment-Dependent Behavior in Crustal Rocks, J, Geophys. Res., 89, 4137-4152, 1984.

E.F.J. von Euw, R.W. Hertzberg and R. Roberts, Delay Effects in Fatigue Crack Propagation, in Stress Analysis and Growth of Cracks, Amer. Soc. Testing Materials, Spec. Tech. Publ. 513, 1972, pp. 230-259.

J. Weertman, Fatigue Crack Propagation Theories, pp. 279-306 of Fatigue and Microstructure, 1978 ASM Materials Science Seminar, 14-15 October, 1978, St. Louis.

R.C. Wei and R.I. Stephens, Fatigue Crack Growth under Spectrum Loads, Amer. Soc. Testing Materials, Spec. Publ. 595, 339 pp., 1975.

O.E. Wheeler, Spectrum Loading and Crack Growth, J. Basic Engrg., March, 1972, pp. 181-186.

T. Yamashita and L. Knopoff, A Model for Precursory Swarms and Seismic Quiescence, Submitted to Science, 1989.

Prof. Thomas Ahrens
Seismological Lab, 252-21
Division of Geological & Planetary Sciences
California Institute of Technology
Pasadena, CA 91125

Prof. Charles B. Archambeau
CIRES
University of Colorado
Boulder, CO 80309

Prof. Muawia Barazangi
Institute for the Study of the Continent
Cornell University
Ithaca, NY 14853

Dr. Douglas R. Baumgardt
ENSCO, Inc
5400 Port Royal Road
Springfield, VA 22151-2388

Prof. Jonathan Berger
IGPP, A-025
Scripps Institution of Oceanography
University of California, San Diego
La Jolla, CA 92093

Dr. Lawrence J. Burdick
Woodward-Clyde Consultants
566 El Dorado Street
Pasadena, CA 91109-3245

Dr. Karl Coyner
New England Research, Inc.
76 Olcott Drive
White River Junction, VT 05001

Prof. Vernon F. Cormier
Department of Geology & Geophysics
U-45, Room 207
The University of Connecticut
Storrs, CT 06268

Prof. Steven Day
Department of Geological Sciences
San Diego State University
San Diego, CA 92182

Dr. Zoltan A. Der
ENSCO, Inc.
5400 Port Royal Road
Springfield, VA 22151-2388

Prof. John Ferguson
Center for Lithospheric Studies
The University of Texas at Dallas
P.O. Box 830688
Richardson, TX 75083-0688

Prof. Stanley Flatte
Applied Sciences Building
University of California
Santa Cruz, CA 95064

Dr. Alexander Florence
SRI International
333 Ravenswood Avenue
Menlo Park, CA 94025-3493

Prof. Henry L. Gray
Vice Provost and Dean
Department of Statistical Sciences
Southern Methodist University
Dallas, TX 75275

Dr. Indra Gupta
Teledyne Geotech
314 Montgomery Street
Alexandria, VA 22314

Prof. David G. Harkrider
Seismological Laboratory
Division of Geological & Planetary Sciences
California Institute of Technology
Pasadena, CA 91125

Prof. Donald V. Helmberger
Seismological Laboratory
Division of Geological & Planetary Sciences
California Institute of Technology
Pasadena, CA 91125

Prof. Eugene Herrin
Institute for the Study of Earth and Man
GeophysicalLaboratory
Southern Methodist University
Dallas, TX 75275

Prof. Robert B. Herrmann
Department of Earth & Atmospheric Sciences
St. Louis University
St. Louis, MO 63156

Prof. Bryan Isacks
Cornell University
Department of Geological Sciences
SNEE Hall
Ithaca, NY 14850

Dr. Rong-Song Jih
Teledyne Geotech
314 Montgomery Street
Alexandria, VA 22314

Dr. Gary McCartor
Mission Research Corporation
735 State Street
P.O. Drawer 719
Santa Barbara, CA 93102 (2 copies)

Prof. Lane R. Johnson
Seismographic Station
University of California
Berkeley, CA 94720

Prof. Thomas V. McEvilly
Seismographic Station
University of California
Berkeley, CA 94720

Prof. Alan Kafka
Department of Geology & Geophysics
Boston College
Chestnut Hill, MA 02167

Dr. Keith L. McLaughlin
S-CUBED
A Division of Maxwell Laboratory
P.O. Box 1620
La Jolia, CA 92038-1620

Prof. Fred K. Lamb
University of Illinois at Urbana-Champaign
Department of Physics
1110 West Green Street
Urbana, IL 61801

Prof. William Menke
Lamont-Doherty Geological Observatory
of Columbia University
Palisades, NY 10964

Prof. Charles A. Langston
Geosciences Department
403 Deike Building
The Pennsylvania State University
University Park, PA 16802

Stephen Miller
SRI International
333 Ravenswood Avenue
Box AF 116
Menlo Park, CA 94025-3493

Prof. Thorne Lay
Department of Geological Sciences
1006 C.C. Little Building
University of Michigan
Ann Arbor, MI 48109-1063

Prof. Bernard Minster
IGPP, A-025
Scripps Institute of Oceanography
University of California, San Diego
La Jolla, CA 92093

Prof. Arthur Lerner-Lam
Lamont-Doherty Geological Observatory
of Columbia University
Palisades, NY 10964

Prof. Brian J. Mitchell
Department of Earth & Atmospheric Sciences
St. Louis University
St. Louis, MO 63156

Dr. Christopher Lynnes
Teledyne Geotech
314 Montgomery Street
Alexandria, VA 22314

Mr. Jack Murphy
S-CUBED, A Division of Maxwell Laboratory
11800 Sunrise Valley Drive
Suite 1212
Reston, VA 22091 (2 copies)

Prof. Peter Malin
University of California at Santa Barbara
Institute for Crustal Studies
Santa Barbara, CA 93106

Dr. Bao Nguyen
GL/LWH
Hanscom AFB, MA 01731-5000

Dr. Randolph Martin, III
New England Research, Inc.
76 Olcott Drive
White River Junction, VT 05001

Prof. John A. Orcutt
IGPP, A-025
Scripps Institute of Oceanography
University of California, San Diego
La Jolla, CA 92093

Prof. Keith Priestley
University of Nevada
Mackay School of Mines
Reno, NV 89557

Prof. Clifford Thurber
University of Wisconsin-Madison
Department of Geology & Geophysics
1215 West Dayton Street
Madison, WS 53706

Prof. Paul G. Richards
Lamont-Doherty Geological Observatory
of Columbia University
Palisades, NY 10964

Prof. M. Nafi Toksoz
Earth Resources Lab
Massachusetts Institute of Technology
42 Carleton Street
Cambridge, MA 02142

Dr. Wilmer Rivers
Teledyne Geotech
314 Montgomery Street
Alexandria, VA 22314

Prof. John E. Vidale
University of California at Santa Cruz
Seismological Laboratory
Santa Cruz, CA 95064

Dr. Alan S. Ryall, Jr.
Center for Seismic Studies
1300 North 17th Street
Suite 1450
Arlington, VA 22209-2308

Prof. Terry C. Wallace
Department of Geosciences
Building #77
University of Arizona
Tucson, AZ 85721

Prof. Charles G. Sammis
Center for Earth Sciences
University of Southern California
University Park
Los Angeles, CA 90089-0741

Dr. Raymond Willeman
GL/LWH
Hanscom AFB, MA 01731-5000

Prof. Christopher H. Scholz
Lamont-Doherty Geological Observatory
of Columbia University
Palisades, NY 10964

Dr. Lorraine Wolf
GL/LWH
Hanscom AFB, MA 01731-5000

Prof. David G. Simpson
Lamont-Doherty Geological Observatory
of Columbia University
Palisades, NY 10964

Prof. Francis T. Wu
Department of Geological Sciences
State University of New York
at Binghamton
Vestal, NY 13901

Dr. Jeffrey Stevens
S-CUBED
A Division of Maxwell Laboratory
P.O. Box 1620
La Jolla, CA 92038-1620

Prof. Brian Stump
Institute for the Study of Earth & Man
Geophysical Laboratory
Southern Methodist University
Dallas, TX 75275

Prof. Jeremiah Sullivan
University of Illinois at Urbana-Champaign
Department of Physics
1110 West Green Street
Urbana, IL 61801

Dr. Monem Abdel-Gawad
Rockwell International Science Center
1049 Camino Dos Rios
Thousand Oaks, CA 91360

Prof. Keiiti Aki
Center for Earth Sciences
University of Southern California
University Park
Los Angeles, CA 90089-0741

Prof. Shelton S. Alexander
Geosciences Department
403 Deike Building
The Pennsylvania State University
University Park, PA 16802

Dr. Ralph Archuleta
Department of Geological Sciences
University of California at Santa Barbara
Santa Barbara, CA 93102

Dr. Thomas C. Bache, Jr.
Science Applications Int'l Corp.
10210 Campus Point Drive
San Diego, CA 92121 (2 copies)

J. Barker
Department of Geological Sciences
State University of New York
at Binghamton
Vestal, NY 13901

Dr. T.J. Bennett
S-CUBED
A Division of Maxwell Laboratory
11800 Sunrise Valley Drive, Suite 1212
Reston, VA 22091

Mr. William J. Best
907 Westwood Drive
Vienna, VA 22180

Dr. N. Biswas
Geophysical Institute
University of Alaska
Fairbanks, AK 99701

Dr. G.A. Bollinger
Department of Geological Sciences
Virginia Polytechnical Institute
21044 Derring Hall
Blacksburg, VA 24061

Dr. Stephen Bratt
Science Applications Int'l Corp.
10210 Campus Point Drive
San Diego, CA 92121

Michael Browne
Teledyne Geotech
3401 Shiloh Road
Garland, TX 75041

Mr. Roy Burger
1221 Serry Road
Schenectady, NY 12309

Dr. Robert Burridge
Schlumberger-Doll Research Center
Old Quarry Road
Ridgefield, CT 06877

Dr. Jerry Carter
Rondout Associates
P.O. Box 224
Stone Ridge, NY 12484

Dr. W. Winston Chan
Teledyne Geotech
314 Montgomery Street
Alexandria, VA 22314-1581

Dr. Theodore Cherry
Science Horizons, Inc.
710 Encinitas Blvd., Suite 200
Encinitas, CA 92024 (2 copies)

Prof. Jon F. Claerbout
Department of Geophysics
Stanford University
Stanford, CA 94305

Prof. Robert W. Clayton
Seismological Laboratory
Division of Geological & Planetary Sciences
California Institute of Technology
Pasadena, CA 91125

Prof. F. A. Dahlen
Geological and Geophysical Sciences
Princeton University
Princeton, NJ 08544-0636

Prof. Anton W. Dainty
Earth Resources Lab
Massachusetts Institute of Technology
42 Carleton Street
Cambridge, MA 02142

Prof. Adam Dziewonski
Hoffman Laboratory
Harvard University
20 Oxford St
Cambridge, MA 02138

Prof. John Ebel
Department of Geology & Geophysics
Boston College
Chestnut Hill, MA 02167

Eric Fielding
SNEE Hall
INSTOC
Cornell University
Ithaca, NY 14853

Prof. Donald Forsyth
Department of Geological Sciences
Brown University
Providence, RI 02912

Prof. Art Frankel
Mail Stop 922
Geological Survey
790 National Center
Reston, VA 22092

Dr. Anthony Gangi
Texas A&M University
Department of Geophysics
College Station, TX 77843

Dr. Freeman Gilbert
Inst. of Geophysics & Planetary Physics
University of California, San Diego
P.O. Box 109
La Jolla, CA 92037

Mr. Edward Giller
Pacific Sierra Research Corp.
1401 Wilson Boulevard
Arlington, VA 22209

Dr. Jeffrey W. Given
Sierra Geophysics
11255 Kirkland Way
Kirkland, WA 98033

Prof. Stephen Grand
University of Texas at Austin
Department of Geological Sciences
Austin, TX 78713-7909

Prof. Roy Greenfield
Geosciences Department
403 Deike Building
The Pennsylvania State University
University Park, PA 16802

Dan N. Hagedorn
Battelle
Pacific Northwest Laboratories
Battelle Boulevard
Richland, WA 99352

Kevin Hutchenson
Department of Earth Sciences
St. Louis University
3507 Laclede
St. Louis, MO 63103

Prof. Thomas H. Jordan
Department of Earth, Atmospheric
  and Planetary Sciences
Massachusetts Institute of Technology
Cambridge, MA 02139

Robert C. Kemerait
ENSCO, Inc.
445 Pineda Court
Melbourne, FL 32940

William Kikendall
Teledyne Geotech
3401 Shiloh Road
Garland, TX 75041

Prof. Leon Knopoff
University of California
Institute of Geophysics & Planetary Physics
Los Angeles, CA 90024

Prof. L. Timothy Long
School of Geophysical Sciences
Georgia Institute of Technology
Atlanta, GA 30332

Prof. Art McGarr
Mail Stop 977
Geological Survey
345 Middlefield Rd.
Menlo Park, CA 94025

Dr. George Mellman
Sierra Geophysics
11255 Kirkland Way
Kirkland, WA 98033

Dr. Richard Sailor
TASC Inc.
55 Walkers Brook Drive
Reading, MA 01867

Prof. John Nabelek
College of Oceanography
Oregon State University
Corvallis, OR 97331

Thomas J. Sereno, Jr.
Science Application Int'l Corp.
10210 Campus Point Drive
San Diego, CA 92121

Prof. Geza Nagy
University of California, San Diego
Department of Ames, M.S. B-010
La Jolla, CA 92093

John Sherwin
Teledyne Geotech
3401 Shiloh Road
Garland, TX 75041

Prof. Amos Nur
Department of Geophysics
Stanford University
Stanford, CA 94305

Prof. Robert Smith
Department of Geophysics
University of Utah
1400 East 2nd South
Salt Lake City, UT 84112

Prof. Jack Oliver
Department of Geology
Cornell University
Ithaca, NY 14850

Prof. S. W. Smith
Geophysics Program
University of Washington
Seattle, WA 98195

Prof. Robert Phinney
Geological & Geophysical Sciences
Princeton University
Princeton, NJ 08544-0636

Dr. Stewart Smith
IRIS Inc.
1616 North Fort Myer Drive
Suite 1440
Arlington, VA 22209

Dr. Paul Pomeroy
Rondout Associates
P.O. Box 224
Stone Ridge, NY 12484

Dr. George Sutton
Rondout Associates
P.O. Box 224
Stone Ridge, NY 12484

Dr. Jay Pulli
RADIX System, Inc.
2 Taft Court, Suite 203
Rockville, MD 20850

Prof. L. Sykes
Lamont-Doherty Geological Observatory
of Columbia University
Palisades, NY 10964

Dr. Norton Rimer
S-CUBED
A Division of Maxwell Laboratory
P.O. Box 1620
La Jolla, CA 92038-1620

Prof. Pradeep Talwani
Department of Geological Sciences
University of South Carolina
Columbia, SC 29208

Prof. Larry J. Ruff
Department of Geological Sciences
1006 C.C. Little Building
University of Michigan
Ann Arbor, MI 48109-1063

Prof. Ta-liang Teng
Center for Earth Sciences
University of Southern California
University Park
Los Angeles, CA 90089-0741

Dr. R.B. Tittmann
Rockwell International Science Center
1049 Camino Dos Rios
P.O. Box 1085
Thousand Oaks, CA 91360

Dr. Gregory van der Vink
IRIS, Inc.
1616 North Fort Myer Drive
Suite 1440
Arlington, VA 22209

William R. Walter
Seismological Laboratory
University of Nevada
Reno, NV 89557

Dr. Gregory Wojcik
Weidlinger Associates
4410 El Camino Real
Suite 110
Los Altos, CA 94022

Prof. John H. Woodhouse
Hoffman Laboratory
Harvard University
20 Oxford Street
Cambridge, MA 02138

Dr. Gregory B. Young
ENSCO, Inc.
5400 Port Royal Road
Springfield, VA 22151-2388

Dr. Ralph Alewine III
DARPA/NMRO
1400 Wilson Boulevard
Arlington, VA 01731-5000

Paul Johnson
ESS-4, Mail Stop J979
Los Alamos National Laboratory
Los Alamos, NM 87545

Mr. James C. Battis
GL/LWH
Hanscom AFB, MA 22209-2308

Janet Johnston
GL/LWH
Hanscom AFB, MA 01731-5000

Dr. Robert Blandford
DARPA/NMRO
1400 Wilson Boulevard
Arlington, VA 87185

Dr. Katharine Kadinsky-Cade
GL/LWH
Hanscom AFB, MA 01731-5000

Eric Chael
Division 9241
Sandia Laboratory
Albuquerque, NM 01731-5000

Ms. Ann Kerr
IGPP, A-025
Scripps Institute of Oceanography
University of California, San Diego
La Jolla, CA 92093

Dr. John J. Cipar
GL/LWH
Hanscom AFB, MA 01731-5000

Dr. Max Koontz
US Dept of Energy/DP 5
Forrestal Building
1000 Independence Avenue
Washington, DC 20585

Mr. Jeff Duncan
Office of Congressman Markey
2133 Rayburn House Bldg.
Washington, D.C. 20515

Dr. W.H.K. Lee
Office of Earthquakes, Volcanoes,
& Engineering
345 Middlefield Road
Menlo Park, CA 94025

Dr. Jack Evernden
USGS - Earthquake Studies
345 Middlefield Road
Menlo Park, CA 94025

Dr. William Leith
U.S. Geological Survey
Mail Stop 928
Reston, VA 22092

Art Frankel
USGS
922 National Center
Reston, VA 22092

Dr. Richard Lewis
Director, Earthquake Engineering & Geophysics
U.S. Army Corps of Engineers
Box 631
Vicksburg, MS 39180

Dr. T. Hanks
USGS
Nat'l Earthquake Research Center
345 Middlefield Road
Menlo Park, CA 94025

James F. Lewkowicz
GL/LWH
Hanscom AFB, MA 01731-5000

Dr. James Hannon
Lawrence Livermore Nat'l Laboratory
P.O. Box 808
Livermore, CA 94550

Mr. Alfred Lieberman
ACDA/VI-OA'State Department Bldg
Room 5726
320 - 21st Street, NW
Washington, DC 20451

Stephen Mangino
GL/LWH
Hanscom AFB, MA 01731-5000

Dr. Frank F. Pilotte
HQ AFTAC/TT
Patrick AFB, FL 32925-6001

Dr. Robert Masse
Box 25046, Mail Stop 967
Denver Federal Center
Denver, CO 80225

Katie Poley
CIA-OSWR/NED
Washington, DC 20505

Art McGarr
U.S. Geological Survey, MS-977
345 Middlefield Road
Menlo Park, CA 94025

Mr. Jack Rachlin
U.S. Geological Survey
Geology, Rm 3 C136
Mail Stop 928 National Center
Reston, VA 22092

Richard Morrow
ACDA/VI, Room 5741
320 21st Street N.W
Washington, DC 20451

Dr. Robert Reinke
WL/NTESG
Kirtland AFB, NM 87117-6008

Dr. Keith K. Nakanishi
Lawrence Livermore National Laboratory
P.O. Box 808, L-205
Livermore, CA 94550

Dr. Byron Ristvet
HQ DNA, Nevada Operations Office
Attn: NVCG
P.O. Box 98539
Las Vegas, NV 89193

Dr. Carl Newton
Los Alamos National Laboratory
P.O. Box 1663
Mail Stop C335, Group ESS-3
Los Alamos, NM 87545

Dr. George Rothe
HQ AFTAC/TGR
Patrick AFB, FL 32925-6001

Dr. Kenneth H. Olsen
Los Alamos Scientific Laboratory
P.O. Box 1663
Mail Stop C335, Group ESS-3
Los Alamos, NM 87545

Dr. Michael Shore
Defense Nuclear Agency/SPSS
6801 Telegraph Road
Alexandria, VA 22310

Howard J. Patton
Lawrence Livermore National Laboratory
P.O. Box 808, L-205
Livermore, CA 94550

Donald L. Springer
Lawrence Livermore National Laboratory
P.O. Box 808, L-205
Livermore , CA 94550

Mr. Chris Paine
Office of Senator Kennedy, SR 315

United States Senate
Washington, DC 20510

Dr. Lawrence Turnbull
OSWR/NED
Central Intelligence Agency, Room 5G48
Washington, DC 20505

Colonel Jerry J. Perrizo
AFOSR/NP, Building 410
Bolling AFB
Washington, DC 20332-6448

Dr. Thomas Weaver
Los Alamos National Laboratory
P.O. Box 1663, Mail Stop C335
Los Alamos, NM 87545

J.J. Zucca
Lawrence Livermore National Laboratory
Box 808
Livermore, CA 94550

Defense Technical Information Center
Cameron Station
Alexandria, VA 22314 (5 copies)

GL/SULL
Research Library
Hanscom AFB , MA 01731-5000 (2 copies)

Defense Intelligence Agency
Directorate for Scientific &
Technical Intelligence
Washington, DC 20301

Secretary of the Air Force (SAFRD)

Washington, DC 20330

AFTAC/CA
(STINFO)
Patrick AFB, FL 32925-6001

Office of the Secretary Defense
DDR & E
Washington, DC 20330

TACTEC
Battelle Memorial Institute
505 King Avenue
Columbus, OH 43201 (Final Report Only)

HQ DNA
Attn: Technical Library
Washington, DC 20305

Mr. Charles L. Taylor
GL/LWH

Hanscom AFB, MA 01731-5000

DARPA/RMO/RETRIEVAL
1400 Wilson Boulevard
Arlington, VA 22209

DARPA/RMO/Security Office
1400 Wilson Boulevard
Arlington, VA 22209

Geophysics Laboratory
Attn: XO
Hanscom AFB, MA 01731-5000

Geophysics Laboratory
Attn: LW
Hanscom AFB, MA 01731-5000

DARPA/PM
1400 Wilson Boulevard
Arlington, VA 22209

Dr. Ramon Cabre, S.J.
Observatorio San Calixto
Casilla 5939
La Paz, Bolivia

Prof. Hans-Peter Harjes
Institute for Geophysik
Ruhr University/Bochum
P.O. Box 102148
4630 Bochum 1, FRG

Prof. Eystein Husebye
NTNF/NORSAR
P.O. Box 51
N-2007 Kjeller, NORWAY

Prof. Brian L.N. Kennett
Research School of Earth Sciences
Institute of Advanced Studies
G.P.O. Box 4
Canberra 2601, AUSTRALIA

Dr. Bernard Massinon
Societe Radiomana
27 rue Claude Bernard
75005 Paris, FRANCE (2 Copies)

Dr. Pierre Mecheler
Societe Radiomana
27 rue Claude Bernard
75005 Paris, FRANCE

Dr. Svein Mykkeltveit
NTNF/NORSAR
P.O. Box 51
N-2007 Kjeller, NORWAY

Dr. Peter Basham
Earth Physics Branch
Geological Survey of Canada
1 Observatory Crescent
Ottawa, Ontario, CANADA K1A 0Y3

Dr. Eduard Berg
Institute of Geophysics
University of Hawaii
Honolulu, HI 96822

Dr. Michel Bouchon
I.R.I.G.M.-B.P. 68
38402 St. Martin D'Heres
Cedex, FRANCE

Dr. Hilmar Bungum
NTNF/NORSAR
P.O. Box 51
N-2007 Kjeller, NORWAY

Dr. Michel Campillo
Observatoire de Grenoble
I.R.I.G.M.-B.P. 53
38041 Grenoble, FRANCE

Dr. Kin Yip Chun
Geophysics Division
Physics Department
University of Toronto
Ontario, CANADA M5S 1A7

Dr. Alan Douglas
Ministry of Defense
Blacknest, Brimpton
Reading RG7-4RS, UNITED KINGDOM

Dr. Roger Hansen
NTNF/NORSAR
P.O. Box 51
N-2007 Kjeller, NORWAY

Dr. Manfred Henger
Federal Institute for Geosciences & Nat'l Res.
Postfach 510153
D-3000 Hanover 51, FRG

Ms. Eva Johannisson
Senior Research Officer
National Defense Research Inst.
P.O. Box 27322
S-102 54 Stockholm, SWEDEN

Dr. Fekadu Kebede
Seismological Section
Box 12019
S-750 Uppsala, SWEDEN

Dr. Tormod Kvaerna
NTNF/NORSAR
P.O. Box 51
N-2007 Kjeller, NORWAY

Dr. Peter Marshal
Procurement Executive
Ministry of Defense
Blacknest, Brimpton
Reading FG7-4RS, UNITED KINGDOM

Prof. Ari Ben-Menahem
Department of Applied Mathematics
Weizman Institute of Science
Rehovot, ISRAEL 951729

Dr. Robert North
Geophysics Division
Geological Survey of Canada
1 Observatory Crescent
Ottawa, Ontario, CANADA K1A 0Y3

Dr. Frode Ringdal
NTNF/NORSAR
P.O. Box 51
N-2007 Kjeller, NORWAY

Dr. Jorg Schlittenhardt
Federal Institute for Geosciences & Nat'l Res.
Postfach 510153
D-3000 Hannover 51, FEDERAL REPUBLIC OF
GERMANY

Prof. Daniel Walker
University of Hawaii
Institute of Geophysics
Honolulu, HI 96822